The Lake-Induced Convection Experiment and the Snowband Dynamics Project

David A. R. Kristovich,[a,n] George S. Young,[b,n] Johannes Verlinde,[b,n] Peter J. Sousounis,[c,n] Pierre Mourad,[d,n] Donald Lenschow,[e,n] Robert M. Rauber,[f,n] Mohan K. Ramamurthy,[f,n] Brian F. Jewett,[f,n] Kenneth Beard,[a,f] Elen Cutrim,[g] Paul J. DeMott,[h] Edwin W. Eloranta,[i] Mark R. Hjelmfelt,[j] Sonia M. Kreidenweis,[h] Jon Martin,[i] James Moore,[k] Harry T. Ochs III,[a,f] David C. Rogers,[h] John Scala,[l,m] Gregory Tripoli,[i] and John Young[i]

ABSTRACT

A severe 5-day lake-effect storm resulted in eight deaths, hundreds of injuries, and over $3 million in damage to a small area of northeastern Ohio and northwestern Pennsylvania in November 1996. In 1999, a blizzard associated with an intense cyclone disabled Chicago and much of the U.S. Midwest with 30–90 cm of snow. Such winter weather conditions have many impacts on the lives and property of people throughout much of North America. Each of these events is the culmination of a complex interaction between synoptic-scale, mesoscale, and microscale processes.

An understanding of how the multiple size scales and timescales interact is critical to improving forecasting of these severe winter weather events. The Lake-Induced Convection Experiment (Lake-ICE) and the Snowband Dynamics Project (SNOWBAND) collected comprehensive datasets on processes involved in lake-effect snowstorms and snowbands associated with cyclones during the winter of 1997/98. This paper outlines the goals and operations of these collaborative projects. Preliminary findings are given with illustrative examples of new state-of-the-art research observations collected. Analyses associated with Lake-ICE and SNOWBAND hold the promise of greatly improving our scientific understanding of processes involved in these important wintertime phenomena.

1. Introduction

Snowstorms that develop each winter as a consequence of cyclones and of destabilization of the lower atmosphere by the Great Lakes have major economic and societal impacts on the midwestern and eastern regions of the United States and Canada. The Great Lakes frequently generate local lake-effect snowstorms, enhancing annual precipitation by as much as 300% compared to regions outside their influence (Scott and Huff 1996). The impacts of these lake-effect storms are illustrated by a recent event that devastated local areas of northeastern Ohio and northwestern Pennsylvania from 9 to 14 November 1996

[a]Illinois State Water Survey, Champaign, Illinois.
[b]The Pennsylvania State University, University Park, Pennsylvania.
[c]University of Michigan, Ann Arbor, Michigan.
[d]University of Washington, Seattle, Washington.
[e]National Center for Atmospheric Research, Boulder, Colorado.*
[f]University of Illinois, Urbana–Champaign, Urbana, Illinois.
[g]Western Michigan University, Kalamazoo, Michigan.
[h]Colorado State University, Fort Collins, Colorado.
[i]University of Wisconsin—Madison, Madison, Wisconsin.
[j]South Dakota School of Mines and Technology, Rapid City, South Dakota.
[k]University Corporation for Atmospheric Research, Boulder, Colorado.
[l]State University of New York College at Brockport, Brockport, New York.
[m]Current affiliation: The Weather Channel, Atlanta, Georgia.
[n]Member of Lake-ICE or Snowband Scientific Steering Committees.
*NCAR is supported by the National Science Foundation.
Corresponding author address: Dr. David A. R. Kristovich, Illinois State Water Survey, 2204 Griffith Drive, Champaign, IL 61820-7495.
E-mail: dkristo@uiuc.edu
In final form 2 August 1999.

(Schmidlin and Kosarik 1999). This climatically rare storm resulted in over $3 million in insured property damages, hundreds of injuries, and eight deaths.

Synoptic-scale cyclones that originate east of the Rocky Mountains and along the western Gulf of Mexico frequently pass across the Great Lakes where they may be strengthened by fluxes of heat and moisture from the lake surfaces (Zishka and Smith 1980; Sousounis and Fritsch 1994; Angel and Isard 1997). As these cyclones track toward the lakes, they produce narrow, heavy swaths of snow, principally from mesoscale precipitation bands north and west of the storm centers within the occluded sector of the cyclone circulation (e.g., Martin 1998, 1999). Kunkel et al. (1999) estimate that cyclone-generated snowstorms have resulted in $1–$3 billion in insured property losses in the United States from 1993 to 1996. One recent intense cyclone in the upper Midwest (1–3 January 1999) resulted in at least 70 deaths, large impacts on transportation, and economic losses (Changnon 1999).

It is hypothesized that lake-effect and cyclone-generated snowstorms are produced by a complex interaction of processes over a wide range of scales. Table 1 lists examples of some lake-effect phenomena on scales defined by Orlanski (1975), and this nomenclature will be used throughout this report. Recent literature has examined a few of the interactions between phenomena on these scales in lake-effect situations. Numerical processes studies, for example, have shown that latent heat release through the development of clouds and snow (microphysical process) significantly increases the depth of lake-effect convection and results in enhanced meso-β-scale snowfall rates (Hjelmfelt 1990). Micro-γ turbulent eddies have been shown to be modulated by larger meso-γ-scale lake-effect boundary layer rolls (Kristovich 1991). Boundary layer convective bands have been found to be influenced by meso-γ-scale circulations generated on the scale of all the Great Lakes (Mann 1999). It is necessary to simultaneously observe all of these scales of phenomena in order to develop a complete understanding of how they interact and build upon one another to be manifested as intense winter snowstorms.

The Lake-Induced Convection Experiment (Lake-ICE) and the Snowband Dynamics Project (SNOWBAND) were developed to observe a wide range of atmospheric phenomena giving rise to heavy snowstorms in the upper U.S. Midwest. The major efforts associated with Lake-ICE focus around developing an understanding of specific processes: 1) What are the mechanisms that control the structure and evolution of meso-γ-scale convective circulations (such as rolls and shore-parallel bands) in boundary layers that are strongly heated from below? 2) What are the interrelationships between these meso-γ-scale circulations and smaller microscale turbulent eddies and cloud and precipitation development? 3) What are the processes by which heat and moisture fluxes from all of the Great Lakes generate atmospheric circulations on the meso-α-scale? SNOWBAND seeks 1) to determine the dynamic and thermodynamic mechanisms associated with heavy precipitation bands in the northwest quadrant of cyclones and 2) to investigate the processes that locally enhance precipitation bands near the Great Lakes during the passage of cyclones.

This paper describes the experimental design and the field operations of Lake-ICE and SNOWBAND and illustrates the usefulness of the state-of-the-art observations taken during the projects through examples of many of the datasets taken.

TABLE 1. Scale nomenclature used in this manuscript (after Orlanski 1975), and some examples in lake-effect snowstorms.

Scale designation	Examples in lake-effect snowstorms
Microphysical	Cloud and precipitation particles, aerosols
Micro γ (< 20 m)	Turbulent eddies, surface-layer eddies, entrainment eddies
Micro β (20–200 m)	Surface-layer lines
Micro α (200 m–2 km)	Thermals, cloud-scale plumes, surface-layer cells
Meso γ (2–20 km)	Boundary layer rolls and cells
Meso β (20–200 km)	Individual lake-scale circulations
Meso α (200–2000 km)	Great Lakes aggregate-scale circulations

2. Background

a. *Lake-ICE*

Operational datasets provide only limited information on the physics of lake-effect snowstorms. Meso-γ-scale precipitation bands, and the micro-γ-scale turbulent circulations within them, are smaller than what can be resolved adequately by stan-

dard surface stations and operational National Weather Service (NWS) sounding sites. These NWS sites are spaced hundreds of kilometers apart in the Great Lakes region. Lake-effect storms are generally quite shallow and often overlaid by high clouds, making observations by surface radar and satellite remote sensing systems difficult. To augment the operational observations, research platforms were deployed to measure meso-α-scale circulations generated by the aggregate effects of all of the Great Lakes, meso-γ-scale lake-effect convective structures, and interactions between boundary layer micro-γ-scale lake-effect convective structures, and interactions between boundary layer micro-γ turbulent eddies and larger circulations, during a number of lake-effect events.

Research efforts to date have provided useful information on the types of meso-γ-scale convective structures common in lake-effect boundary layers. Kelly (1986) and Kristovich and Steve (1995) found that lake-effect convection tends to organize into two types of meso-γ-scale convective structures: 1) widespread convection, most often with multiple wind-parallel bands, and 2) single or double bands parallel to the long axis of the lake. The latter study reported that the most frequent cloud structure over Lake Michigan was widespread wind-parallel bands, occurring on about 20% of December and January days on average, and accounting for nearly 60% of lake-induced cloudiness during those months. Kelly (1984) found that wind-parallel bands of convection, associated with boundary layer rolls, were generally associated with strong cross-lake winds (westerly component winds over Lake Michigan). However, conditions in which rolls were observed were not theoretically conducive to these convective patterns (Kristovich 1993). Bands of convection parallel to the long axis of a Great Lake tend to develop in situations where the cross-lake component of the synoptic-scale wind velocity is small and when air–lake temperature differences are high (e.g., Lavoie 1972; Passarelli and Braham 1981; Niziol 1987; Hjelmfelt 1990). However, the temporal and spatial evolution of these bands is particularly difficult to predict, since little is known about how these bands are influenced by variations in surface and synoptic-scale forcing, gravity waves, wind shear, and cloud and precipitation development. Lake-ICE seeks to better understand how the structure of snow-producing meso-γ convective structures evolve in lake-effect snowstorms.

Investigations of how the structure of meso-γ-scale boundary layer convective circulations affect boundary layer fluxes have been difficult to conduct. Nevertheless, there is increasing evidence that the meso-γ-scale organization of convection has a significant impact on the spatial variation of micro-γ-scale turbulent eddies and thermals (e.g., LeMone 1976; LeMone and Pennell 1976; Agee and Hart 1990; Dalu and Pielke 1993; Moyer and Young 1991; Mourad 1996). One of the major goals of Lake-ICE is to develop a better understanding of interactions between rolls and fluxes throughout the depth of the boundary layer.

Satellite-based synthetic aperture radar (SAR) imagery has been used to detect the presence of organized circulation structures in the marine atmospheric surface layer under a variety of conditions (reviewed in Mourad 1999). These observations build on past work, which showed that rolls and gust microfronts can modulate surface layer fluxes (e.g., LeMone 1976; Mahrt and Gibson 1992). Ultimately, the impacts of heat and moisture transport from the surface layer depend on the rate at which heat, moisture, and momentum are transferred vertically by multiscale circulations throughout the mixed layer. For example, rolls have been found to influence the location of cloud and precipitation development, modulate micro-γ-scale turbulent eddies, and control the locations of micro-β-scale convective turrets (e.g., Streten 1975; LeMone and Pennell 1976; Kelly 1984; Christian and Wakimoto 1989; Kristovich 1993, 1995; Kristovich and Braham 1998).

Finally, the rate at which the boundary layer grows across the lake (i.e., its Lagrangian rate of change) will depend largely on the rate at which air is entrained into the boundary layer. Most observational evidence of whether entrainment occurs primarily through engulfment of large parcels of ambient air or by interfacial shear-induced turbulent mixing has been limited to boundary layers with weak thermal forcing from below (e.g., Melfi et al. 1985; Atlas et al. 1986; Moeng and Sullivan 1994). These processes, especially engulfment, are thought to be related to cloud-top entrainment instability (Shy and Breidenthal 1990; MacVean and Mason 1990; Khalsa 1993). This relationship is thought to exist because the rate at which air is entrained into the boundary layer depends on the amount of turbulence that is consumed mixing air into the boundary layer (Wang and Albrecht 1994). In the limiting case where no turbulence is consumed to enhance boundary layer growth, the boundary layer is said to grow solely by encroachment. The key question arising from these studies is, What environmental, cloud-scale, and turbulence dynamics effects

control the degree to which the rate of entrainment exceeds that due to encroachment? Lake-ICE will aid in studies of these processes in cases with intense surface heating of the boundary layer.

The overall impact of the boundary layer processes described above is to modify the meso-α-scale circulations and their thermodynamic characteristics. These modifications involve a dynamical adjustment process that links meso-β lake forcing to larger meso-α responses (e.g., Yuen and Young 1986). Indeed, it has been known for some time that the Great Lakes affect the movement and evolution of synoptic-scale weather systems (e.g., Cox 1917; Petterssen and Calabrese 1959). A numerical modeling effort by Sousounis and Fritsch (1994) demonstrated that the Great Lakes not only affect regional weather systems, but may also be responsible for affecting weather over a much larger region (e.g., mid-Atlantic Coast, southeastern Canada, New England). Since cold air outbreaks occur regularly throughout the winter season, the lakes have a significant influence on regional climate (Bates et al. 1993, 1995; Scott and Huff 1996; Weiss and Sousounis 1999). Despite these significant and far-reaching effects, a clear understanding of how and when the Great Lakes impact regional weather and climate does not exist. Studies associated with Lake-ICE utilize modeling and observational techniques to investigate the extent to which the Great Lakes alter regional circulations.

b. SNOWBAND

While cyclones are reasonably well observed in the central United States, processes thought to be responsible for associated heavy snowbands (such as frontal lifting, ageostrophic circulations during frontogenesis, and conditional symmetric instability) occur on scales below the resolution of the national rawinsonde network. Three-dimensional circulations at these scales cannot be determined with existing operational resources. The Snowband Dynamics Project examined the development of snowbands associated with wintertime cyclones. Frontal structures and associated frontal circulations are modified sharply in the northwest sector of cyclones by strong deformation flow. Often extremely heavy precipitation falls within an approximately 200-km-wide swath in the northwest quadrant of cyclones as they progress eastward from the Rocky Mountains to the Great Lakes region. Strong surface pressure gradients and winds within this cold sector of the storm frequently produce blizzard conditions. When viewed with radar, snowstorms in the northwest quadrant of cyclones often consist of one or more bands of heavy snow, typically 500–200 km wide, generally oriented parallel to the midtropospheric shear vector. Isentropic trajectory analyses have shown that several air masses, with different thermal and moisture characteristics, converge in this region (e.g., Kreitzberg and Brown 1970; Schultz and Mass 1993; Martin 1998, 1999). Although it is generally recognized that the dominant mechanisms for precipitation band formation include slantwise ascent due to frontal lifting, ageostrophic circulations during frontogenesis, and conditional symmetric instability, the vertical structure and dynamics of snowbands in the northwest quadrant of cyclones are still not well understood, both because the crossband width is below the current rawinsonde network resolution and because no systematic scientific study has been conducted to obtain the necessary observations. The Snowband Dynamics Project was designed to document and understand the mechanisms associated with the formation of these heavy precipitation bands.

When cyclones follow a track south of Lake Michigan, a strong easterly flow develops over the lake that can lead to lake-induced clouds and snowfall along the western shore. Simultaneously, snow is produced by the mechanisms discussed in the previous paragraph within the larger-scale circulations associated with the cyclone. Heavy snowstorms west of Lake Michigan can result from this interaction of lake-effect and frontal processes, as boundary layer fluxes of heat and moisture from the lake modify the stability profile and existing frontal structure, and the mid- and upper-tropospheric clouds seed the lower lake-induced clouds. The second objective of SNOWBAND was to investigate the processes that locally enhance precipitation bands along the western side of Lake Michigan during the passage of cyclones south of the lake.

By combining the resources available for all of these investigations, Lake-ICE and SNOWBAND collected a comprehensive dataset that will allow for investigations of the simultaneous physical processes that result in heavy snow in the midwestern and northeastern regions of the United States. Scientific investigations using these datasets will increase knowledge of atmospheric–marine interactions, mesoscale circulations, cloud–circulation interactions, and turbulent transport in convective marine boundary layers. In addition, these investigations will allow for a better understanding of mesoscale precipitation systems embedded in cyclonic storms.

3. Experimental design

Lake-ICE and SNOWBAND incorporated a variety of airborne and ground-based sensor systems to examine wintertime snow-producing phenomena (Table 2). Data collected by the research platforms during a number of intensive operations periods (IOPs), in combination with operational datasets, allow for detailed investigations of lake-effect boundary layer convective structures, turbulence, and cloud and precipitation microphysical characteristics, as well as mesoscale precipitation and thermodynamic characteristics of cyclones. There were three major regions of focus in the field experiments: 1) surface, airborne, and remote sensing observations over and near Lake Michigan; 2) sounding observations taken in southeastern Canada; and 3) airborne and sounding observations across the northwest regions of cyclones.

a. Platforms over and near Lake Michigan

Platforms deployed near Lake Michigan in support of Lake-ICE and SNOWBAND operations (Fig. 1) included two research aircraft [National Center for Atmospheric Research (NCAR) Electra (N308D) and University of Wyoming King Air (N2UW)], three NCAR integrated sounding systems (ISS), the Pennsylvania State University Cloud Observing System (PSU COS; Albrecht et al. 1991), and the University of Wisconsin volume imaging lidar (UW VIL). Locations of the ISS sites were chosen to provide high spatial resolution observations of boundary layer growth around Lake Michigan as well as to enhance the NWS operational sounding network.

The ISS sites monitored synoptic-scale and meso-α-/meso-β-scale evolution of the lower troposphere upwind and downwind of Lake Michigan with several components: 1) a balloon-borne navaid sounding sys-

TABLE 2. Research datasets taken during Lake-ICE and SNOWBAND. Abbreviations: National Center for Atmospheric Research (NCAR), integrated sounding system (ISS), cross-chain long-range navigation (loran) atmospheric sounding system (CLASS), Surface and Sounding Systems Facility (SSSF), Research Aviation Facility (RAF), Remote Sensing Facility (RSF), range–height indicator (RHI), plan position indicator (PPI), Pennsylvania State University–NCAR Mesoscale Model (MM5), nonhydrostatic modeling systems (NMS).

Research dataset	Data resol./product type	Data source
NCAR ISS/CLASS including sounding, profiler, and sfc met observations	• Temporal: 1.5–6-h variable (CLASS) • Vertical resolution (CLASS) 10 s (approximately 50 m) • 1 min (surface observations)	NCAR/SSSF
NCAR Electra	• Selected IOPs • Temporal: 0.05–1 s	NCAR/RAF
NCAR ELDORA (airborne radar)	• Spatial: 75-m gate spacing, variable scan strategies	NCAR/RSF
University of Wyoming King Air multiple parameters	• Selected IOPs • Temporal: 0.1–1 s	University of Wyoming
University of Wisconsin volume imaging lidar	• Selected IOPs • Spatial: 15-m range resolution, RHI, PPI, volume scan modes	University of Wisconsin
Cloud Observing System including microwave radiometer, laser ceilometer, CLASS radiosonde, and 94-Ghz cloud radar	• Selected IOPs • Spatial: Radar has 15-m height resolution, other instruments variable	The Pennsylvania State University
Mesoscale research models (University of Michigan - MM5, University of Wisconsin - NMS)	• Nested grids • Temporal: 6-h time increments	University of Michigan University of Wisconsin

tem, 2) an enhanced surface observing station, 3) a 915-MHz Doppler clear-air wind profiling radar, and 4) a radio acoustic sounding system. Sondes were generally launched at 90-min to 3-h time intervals on flight days. The other ISS components operated continuously. The ISS were deployed at Sheboygan, Wisconsin, and Muskegon and Greenville, Michigan.

The PSU COS, consisting of the PSU 94-GHz cloud radar, a laser ceilometer, and a Global Positioning System radiosonde system, was deployed at the Great Lakes Environmental Research Laboratory Lake Michigan Field Station in Muskegon. This observation site was on the downwind shore during Lake-ICE operations, allowing for high vertical and temporal resolution observations of cloud and precipitation microphysical characteristics and turbulence in the cloud layer near the eastern shore of Lake Michigan. The UW VIL deployed at Sheboygan provided information on clear-air circulation structures over the upwind portion of Lake Michigan during many Lake-ICE operational days.

The primary Electra instrumentation included the Electra Doppler radar (ELDORA); the scanning aerosol backscatter lidar; and the standard in situ dynamical, thermodynamical, microphysical, and radiation sensors (NCAR Research Aviation Facility 1997). Additional NCAR supplied instruments were incorporated to achieve the Lake-ICE goals: the radar altimeter, fast-response Lyman-alpha hygrometer, an Ophir III radiometric thermometer, fast and slow ozone monitors, an aerosol spectrometer, cloud droplet spectrum probes, forward scattering spectrometer probe [(FSSP)—300, 260X], and hydrometeor probes (2D-C, 2D-P). User-supplied scientific payloads included a continuous-flow diffusion ice nucleus chamber provided by Rogers et al. (2000, manuscript submitted to *J. Atmos. Oceanic Technol.*), a counterflow virtual impactor (Twohy et al. 1997), a TSI Electrometer Model 3068, and a cryogenic air sample collector. King Air instrumentation included in situ, microphysical and radiation sensors. Both aircraft made extensive use of their high quality navigational and communications systems for the coordination of King Air flight legs with those of the Electra.

The experimental design of aircraft operations during Lake-ICE was to conduct coordinated flights to provide simultaneous observations within the boundary layer parallel to, and orthogonal to, the mean flow. During the portion of each Lake-ICE mission when the King Air was on station over Lake Michigan, the Electra flew legs designed to provide optimal ELDORA measured meso-γ-scale structure of lake-induced convection while the King Air conducted flight tracks that were designed to study the mesoscale–microscale–microphysics interrelationships within such meso-γ-scale structures (Fig. 2). The Electra flew along-wind legs across Lake Michigan at altitudes that minimized problems with ELDORA observations due to second-trip and sidelobe echoes from the lake surface. When snow was light enough to permit visual flight rules operation, the Electra flew at the minimum safe altitude, generally 120–190 m above the lake. When snow was intense enough to require instrument flight, the Electra flew at about 580 m above the lake, making use of attenuation by the snow to eliminate second-trip contamination. Both approaches were successful, as will be shown in section 5a. While the Electra

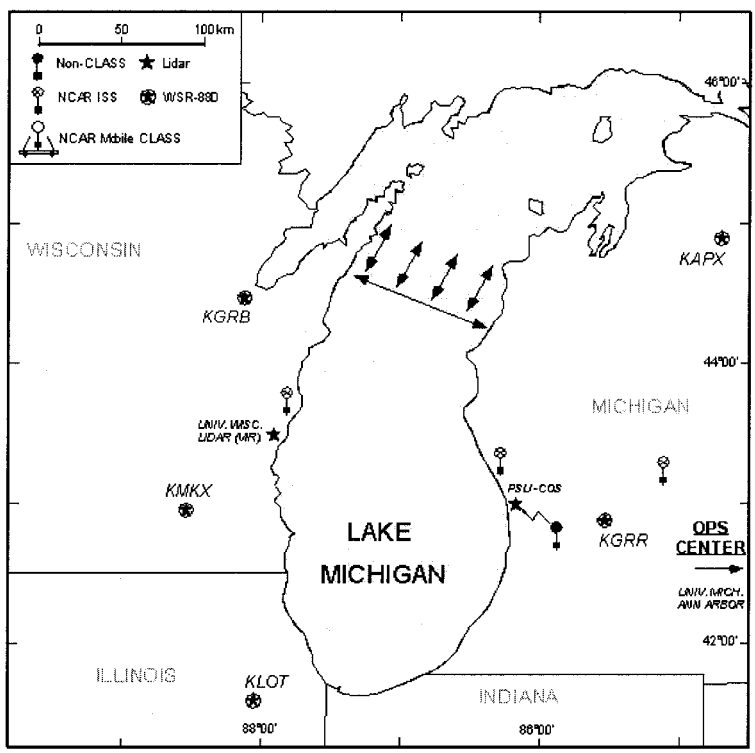

FIG. 1. Locations of facilities in the vicinity of Lake Michigan used during Dec 1997 and Jan 1998. Arrows denote the approximate locations of flight legs conducted by the NCAR Electra (single line oriented WNW–ESE) and the University of Wyoming King Air (four lines oriented SW–NE) on 13 Jan 1998.

was executing these low-level legs, the King Air performed a set of four crosswind stacks, spaced across the width of Lake Michigan in the zone of ELDORA coverage. Each stack consisted of five 30-km legs with the top two flight levels as close as possible to the capping inversion to evaluate entrainment (i.e., one approximately 50 m above cloud top and the other approximately 50 m below cloud top). The other flight levels were selected to sample key heights in the vertical flux profile: the midcloud layer, cloud base, and as close as possible to the lake surface.

After each coordinated Lake-ICE mission, the King Air refueled near the downwind shore of the lake and then proceeded alone to fly in-cloud racetracks over the PSU COS or return directly to the base of flight operations, Willow Run Airport in Ypsilanti, Michigan. During this period, the Electra would execute a set of 60-km crosswind legs similar to those performed by the King Air over the middle or downwind portions of the lake before returning to Willow Run. The total flight duration for each of the aircraft missions was 6–7 h.

Additionally, a small number of single-aircraft missions were flown to achieve special scientific goals. On 11 January 1998, the King Air flew a solo mission on a day with convective boundary layer growth to 1) collect a high spatial resolution dataset on cloud microphysical properties above the PSU COS, 2) detail the north–south variation of boundary layer characteristics and surface fluxes, and 3) provide in situ observations near the UW VIL and surface flux buoy. The Electra conducted a set of divergence/entrainment circles (Lenschow et al. 1999) on 19 January 1998 in a partially coupled stratocumulus-topped convective boundary layer and an SAR intercomparison mission on 18 January 1998 in weak synoptically disturbed lake-effect convection.

Satellite-based SAR images were archived to obtain information on lake surface characteristics over the time period of field operations. The lake surface is roughened by wind within the atmospheric surface layer via the production of gravity–capillary waves (Dorman and Mollo-Christensen 1973; Kahma and Donelan 1987; Caulliez et al. 1998). This surface roughening, in turn, alters backscatter radar signals via Bragg scattering for grazing angles between 20° and 70° (Plant 1990). The SAR can therefore be used to obtain information on the effects of atmospheric surface layer phenomena. Processes observed by SAR in past studies include cyclones, warm fronts, atmospheric gravity waves, atmospheric micro-γ-scale turbulence, meso-γ-scale roll vortices and cellular convection within cold air outbreaks, and boundary layer convection (Johannessen et al. 1991; Mourad 1996; Mourad and Walter 1996; Sikora et al. 1995; Vachon et al. 1998; reviewed in Mourad 1999). One of the goals of Lake-ICE is to make use of SAR imagery as an analysis tool for mesoscale distribution of boundary layer turbulence over Lake Michigan, particularly within cold air outbreaks.

Figure 3 gives an example of an SAR image taken by the Canadian satellite *RADARSAT, International* of the southern half of Lake Michigan on 18 January 1998. Features of note include a ribbon of ice in the southeast corner of the lake and a set of image-acquisition artifacts in the form of multiple horizontal lines. Of geophysical interest here are the subtle, "puffy" features predominantly in the southwest quadrant of the lake. Similar radar backscatter structure has been shown previously to be related to atmospheric boundary layer turbulence structures (Mourad 1996; Sikora et al. 1995). Coincident with this image are flights of the King Air and Electra, conducted to measure atmo-

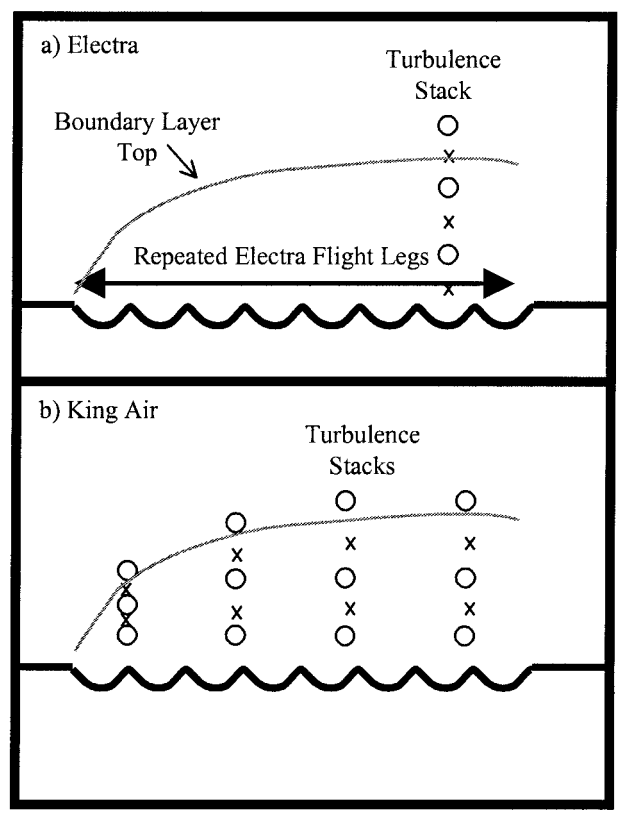

FIG. 2. Vertical cross-section view of Lake-ICE flight plans conducted on most of the Lake-ICE operational days. Circles and "X's" denote flight legs into, and out of, the cross section.

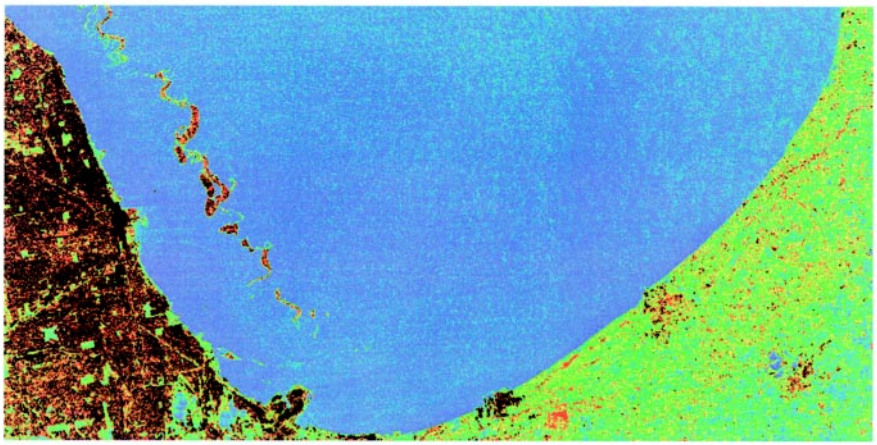

FIG. 3. Synthetic aperture radar image from *RADARSAT, International,* of the southern part of Lake Michigan during Lake-ICE. This image was taken at 1151 UTC on 18 Jan 1998. (Copyright 1998, Canadian Space Agency.)

spheric turbulence characteristics. Determination of a strong correlation between structure in radar backscatter and turbulence using this combination of in situ and remotely sensed data may ultimately allow SAR to quantify atmospheric turbulence and associated fluxes remotely.

b. Lake-ICE platforms in southeastern Canada

Past studies indicate that the Great Lakes can have a large impact on regional weather systems, particularly on cyclones passing through the region (e.g., Sousounis and Fritsch 1994; Angel and Isard 1997). Of particular interest to Lake-ICE investigators was the development of meso-α-scale circulations spawned by the aggregate effects of the Great Lakes. Sousounis (1997) characterized these circulations as mesoscale aggregate vortices (MAVs). Numerical modeling results from this study indicate that the spatial resolution of the operational sounding networks in the United States and Canada would likely not be able to resolve the structure and evolution of MAVs.

Figure 4 shows the locations of five NCAR CLASS sites and one National Severe Storms Laboratory mobile CLASS site deployed to fill gaps in the operational sounding network. The sounding sites essentially doubled the operational horizontal resolution of wind measurements in an area of the northeast of the Great Lakes, shown by these modeling studies to be a common region for the development of MAVs. The CLASS units obtained data on wind, temperature, relative humidity, and pressure at vertical resolutions sufficient for delineating the structure of MAVs. Sounding data were collected at these sites typically at 3-h intervals over approximately 9 days during Lake-ICE. These unprecedented observations will allow for study of the development and evolution of MAVs.

c. Snowband dynamics platforms

The observational strategy to meet SNOWBAND objectives made use of the ELDORA radar, dropsonde measurements, and standard wind, thermodynamic, and microphysical instrumentation on board the NCAR Electra aircraft. In addition, high-resolution soundings and detailed vertical wind profiles from ISS systems were obtained in the vicinity of Lake Michigan. The objective of the observational strategy was to document the 3D kinematic structure of the heavy snowbands while measuring the cross-band thermodynamic and microphysical structure. ELDORA's effective range for dual-Doppler recovery of winds was nominally 40 km on either side of the aircraft at altitudes flown for SNOWBAND cases (nominal distance will depend on such factors as aircraft height and altitude, depth of the precipitation layer, and scatterer characteristics). The radial veloci-

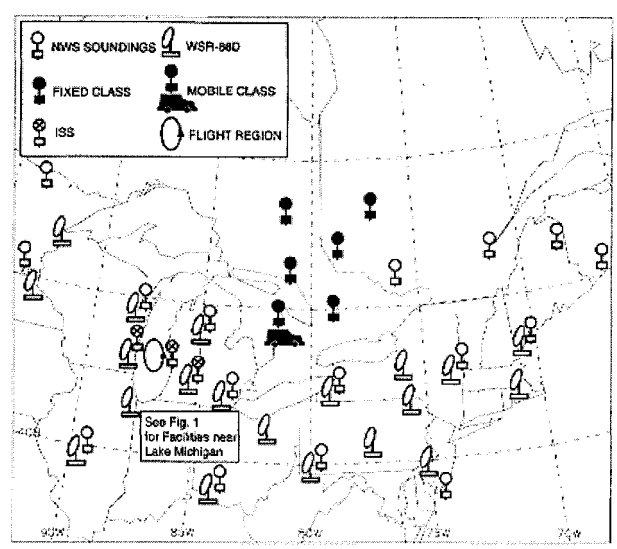

FIG. 4. Locations of CLASS and mobile CLASS sounding sites for Lake-ICE. Open symbols indicate operational observation sites, and filled symbols indicate special project data collection sites. For reference, the approximate location of research aircraft flights is shown over Lake Michigan.

ties from the fore and aft radars were obtained with 150-m gate spacing and along-track resolution of about 325 m. Dropsondes were deployed approximately every 20 km across the bands. Similar strategies were employed during one case of lake enhancement of a deeper cyclonic system. Typically three to four low-level [~1 km above mean sea level (MSL)] passes were flown to obtain the Doppler wind measurements. In addition, a high-level (~7 km MSL) pass was made during the deployment of the dropsondes. Approximately 20 dropsonde launches were made during each flight. CLASS soundings were launched at 90-min frequency at the U.S. sites during the intensive operations periods.

During the project, high-resolution measurements of wind and thermodynamic fields were obtained in the vicinity of the occlusion sector of two cyclones that produced heavy snowfall. At least one of these cases also had a significant enhancement of snowfall on the west side of the lake. In addition, west shore lake enhancement occurred in a third case associated with an approaching cyclone. A description of these cyclones and some initial analyses are presented in section 5c.

d. Operational data

A wide variety of data were required for project operations and were archived for use in analyses. Table 3 summarizes the operational datasets collected and the sources. Except where noted, these data are in the Lake-ICE archive managed by the University Corporation for Atmospheric Research Joint Office for Scientific Support (JOSS).

4. Field project operations

The Lake-ICE and SNOWBAND Operations Center consisted of a communications center, a forecast center, an analysis center, and a briefing room located within the Atmospheric, Oceanic, and Space Sciences Department at the University of Michigan. This location was chosen because of its close proximity to the Willow Run Airport, where the Electra and King Air were based, and because of the department's supportive infrastructure (particularly access to weather data, products, and specialized models) for these activities.

a. Operations center functions

The Lake-ICE and SNOWBAND Operations Center staff was responsible for 1) operational implementation of scientific missions set forth by the steering committee; 2) monitoring the status of all project facilities; 3) supporting voice, data, and facsimile interactions with all participants and facilities involved in the project; and 4) project forecasting. Operational support was provided primarily by JOSS, the University of Michigan, and the University of Wisconsin.

The daily schedule was based on the expected Lake-ICE and SNOWBAND flight and sounding routines and on the need for project coordination. A daily planning meeting was held each day at 1500 LST and included an overview of project facility status, a weather update and forecast, and determination of the following day's operations. Decisions made in the meeting were communicated to project participants via telephone recording and a Web-based online catalog, developed by JOSS. Preflight and pilot briefings were conducted on anticipated flight days. Close coordination between Lake-ICE and SNOWBAND activities was crucial to ensure that participants had sufficient opportunities to address project objectives through acquisition of essential research data. Project coordination was achieved through weekly joint strategic planning meetings. A Joint Operations Committee consisting of representatives from Lake-ICE and from SNOWBAND was formed to resolve any major conflicts (but never met).

b. Forecasting

The forecast center provided daily forecasts, nowcasts, and short-term outlooks during operational periods, and advised the operations director of changing weather conditions that could affect operations. A unique aspect of the forecasting operation was the regular participation of the NWS Forecast Office in White Lake, Michigan.

Two mesoscale research models, run at the University of Michigan and at the University of Wisconsin, supported project forecasting efforts. The University of Michigan provided forecasting support for Lake-ICE utilizing the National Center for Atmospheric Research–Pennsylvania State University (NCAR–PSU) Mesoscale Model MM5 (version 2). Two pairs of runs were made each day, corresponding to the 0000 UTC and 1200 UTC cycles. Each pair consisted of a with-lake and a no-lake simulation. The model configuration utilized 90/30 km two-way nested domains with 25 vertical levels. The inner domain covered the entire Great Lakes region (e.g., 41×31 points). The 30-km fine mesh was run to 30 h, and the 90-km coarse mesh was run to 48 h. The no-lake simulation excluded the Great Lakes as described in Sousounis and Fritsch (1994). The no-lake model used

TABLE 3. Operational datasets archived during Lake-ICE and SNOWBAND. Abbreviations: Surface and Sounding Systems Facility (SSSF), Next Generation Weather Radar (NEXRAD), National Climatic Data Center (NCDC), National Oceanic and Atmospheric Administration (NOAA), and Federal Aviation Administration (FAA).

Operational dataset	Data resolution/product type	Data source
Composite rawinsonde data—entire United States plus field operations sites	• All soundings launched between 1 Dec 1997 and 26 Jan 1998; 6-s vertical resolution • Temporal resolution: 12 hourly, Variable 1.5–6 hourly (field sites)	• JOSS • NCAR/SSSF • The Pennsylvania State University
Network profiler data	• Winds, control, surface, and moments data • Spatial: selected stations • Temporal: 1 hourly	• NCDC • NOAA
Aircraft communications and reporting system (commercial aircraft observations)	• All data between 1 Dec 1997 and 26 Jan 1998 • Spatial: North America • Temporal: 6–30 s	• NOAA/Forecast Systems Laboratory
Automated surface observing system and automated weather observing system	• Spatial: All sites in eastern and central United States • Temporal: 5 min, 20 min	• JOSS, from NOAA, FAA
WSR-88D (NEXRAD) radar level II archive	• Spatial: Selected sites in upper Midwest • Temporal: all data during IOP events	• NCDC
NEXRAD Information Dissemination Service products	• Products: Regional and national composites, reflectivity, velocity, as well as other composite and precipitation products for 18 selected radars in the Midwest • Temporal: 6–10 min	• University of Illinois from Weather Services International
GOES-8 regional visible, infrared, and water vapor wavelengths	• Spatial: 1 km visible; 4 km infrared; 8 km water vapor • Temporal: 30 min, 1–5 min (Rapid Scan, Super Rapid Scan)	• University of Wisconsin Space Science and Engineering Center
Other supplemental Midwest data including surface stations, Great Lakes surface temperatures, and snow observations	• Variable	• Multiple
Canadian soundings	• Spatial: Selected stations • Temporal: 12 hourly • Vertical resolution: 6 s	• Atmospheric Environment Service
Canadian surface observations	• Spatial: selected stations • Temporal: hourly	• Atmospheric Environment Service
Operational model output	• Temporal: 6–12-h time steps in forecast	• NOAA

only a 90-km grid with 25 vertical levels and was run to 48 h.

Forecasting support was also provided by the University of Wisconsin Nonhydrostatic Modeling System (UW NMS). The UW NMS used a three-grid configuration with the second grid covering all the upper Midwest and an inner grid encompassing a 400 km × 400 km domain centered on southern Lake Michigan. The horizontal resolutions of the inner grids were 60 and 20 km. The UW NMS used 30 vertical

levels, with a vertical grid spacing of 200 m for the first five grid boxes near the ground, stretching gradually to a minimum resolution of 1000 m, above which the grid spacing was held constant to the model top of 16 km.

c. Data management activities

Lake-ICE and SNOWBAND employed a comprehensive data management strategy to help ensure that special research data and supporting operational datasets were available to all participants and the larger scientific community. The project steering committees specified a list of data protocols that formed the basis of the data management strategy. The protocols addressed areas of data processing and quality control, sharing of data among principal investigators and with the outside community, timelines of data submissions, and responsibilities and organization of the data archive. The JOSS utilized a questionnaire to get participant feedback on data-related needs before the field efforts began, which permitted timely exchange of quality data during the project.

The JOSS utilized the World Wide Web to provide online catalog access of operational data and preliminary research data for scientists in the field. The catalog allowed data entry (operations and status summaries, flight summaries, certain operational data, etc.), data browsing (listings and plots), and data distribution to interested parties. Several of the participating groups, including the University of Michigan, the University of Wisconsin, the University of Illinois, and NCAR, provided specialized model output, radar products, and other preliminary data analysis products using existing or new Web pages. These sites were all interconnected and provided accessibility to important data required for planning and operational decision making.

5. Observations and results

The project consisted of nine intensive operations periods (IOPs) during the 42 days of field operations. IOPs were defined as those with continuous observations made by any of the research observing systems and often lasted several days. A summary of each IOP, associated scientific objectives, and active research platforms (aircraft flights, sounding launches, etc.) is provided in Table 4. This section gives examples of data collected, and some preliminary results, from two cases during Lake-ICE and from one SNOWBAND case.

a. Lake-ICE example, 10–12 January 1998

CLASS soundings were taken in southeastern Canada to learn more about lake aggregate effects (Sousounis and Fritsch 1994) and mesoscale aggregate vortices (Sousounis 1997), which develop during cold air situations over the Great Lakes. Previous deficiencies in the horizontal resolution of the upper-air ob-

TABLE 4. Lake-ICE/SNOWBAND intensive operations periods.

IOP	Dates	Project	Aircraft	ISS*	CLASS*	COS/VIL
1	4–6 Dec 1997	Lake-ICE	Electra, King Air	3-h	3-h	Yes/Yes
2	9–11 Dec 1997	SNOWBAND	Electra	None	None	No/No
3	13–14 Dec 1997	Lake-ICE	None	3-h	3-h	No/Yes
4	20–21 Dec 1997	Lake-ICE	Electra, King Air	3-h	None	Yes/Yes
5	8 Jan 1998	SNOWBAND	Electra	90-min	None	No/No
6a	10–12 Jan 1998	Lake-ICE	Electra, King Air	90-min	3-h	Yes/Yes
6b	13–15 Jan 1998	Lake-ICE	Electra, King Air	90-min	3-h	Yes/Yes
7	18 Jan 1998	Lake-ICE	Electra, King Air	90-min	None	Yes/Yes
8a	19–20 Jan 1998	Lake-ICE	Electra, King Air	90-min	3-h	Yes/Yes
8b	20 Jan 1998	Lake-ICE	Electra, King Air	90-min	None	Yes/No
9	21–22 Jan 1998	SNOWBAND	Electra	90-min	None	No/No

*Balloon launch frequency is listed.

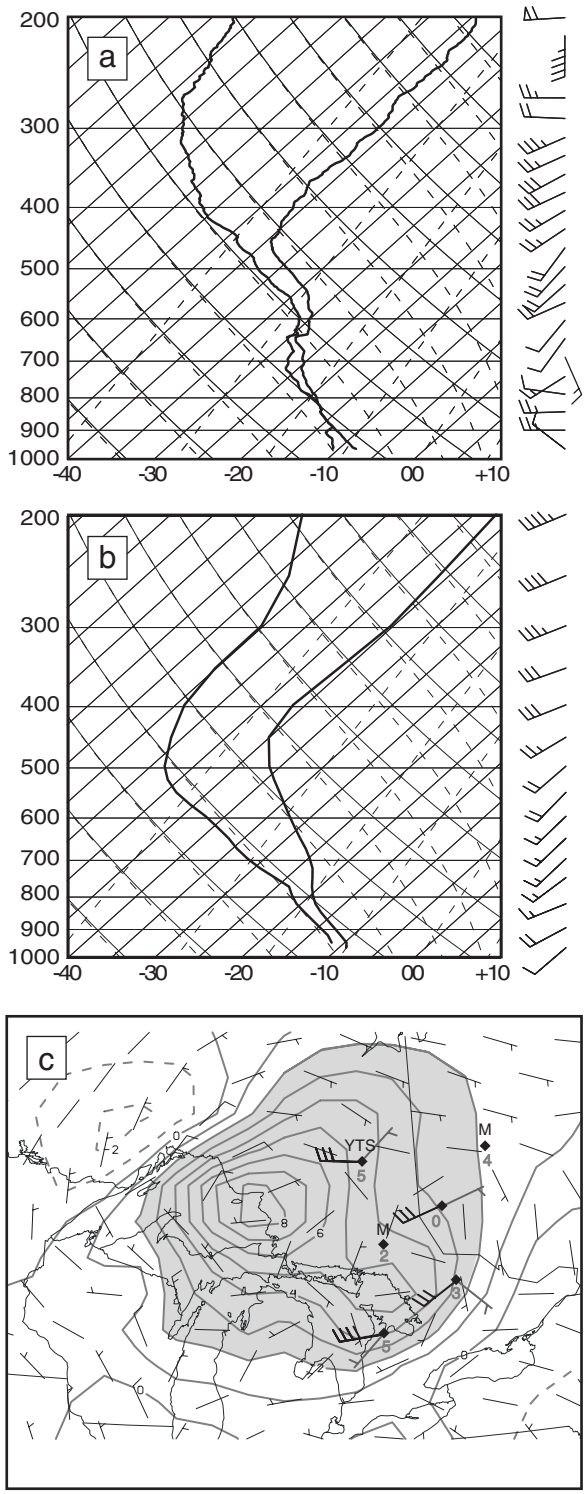

FIG. 5. Sounding information valid 0000 UTC 11 Jan 1998. (a) CLASS sounding for Timmons (YTS). (b) 24-h WL model sounding for Timmons from 90-km NCAR–PSU MM5 grid. (c) CLASS winds (heavy black barbs), CLASS–NL wind perturbations (heavy gray barbs), and temperature perturbations (°C; heavy gray numbers) at 900 hPa. Missing wind information indicated by "M." WL–NL wind (light barbs) and temperature (light contours) perturbations at 900 hPa. Shaded region indicates WL–NL temperature perturbation > 2°C.

servational network have precluded the observational documentation of these effects and were a primary motivating factor for this aspect of Lake-ICE.

A classic lake aggregate case developed during 10–12 January 1998 (IOP 6a). Cold air had overspread the Great Lakes region during 9 and 10 January and was well established by 0000 UTC 11 January. The large-scale flow was characterized by a synoptic-scale surface low (central sea level pressure ~1002 hPa) located near Hudson Bay, a surface trough extending southwestward over the lakes region, and a 500-hPa low (~510 dam) centered 500 km north of Sault Ste. Marie, Michigan. The 1000–500-hPa thicknesses were thus around 510 dam with a 850-hPa temperatures between −15° and −10°C [e.g., the classic lake-effect criteria by Rothrock (1969) were satisfied]. Light to moderate snow was falling throughout the region at the time, especially near the lake shores.

Figure 5a shows a CLASS sounding from Timmins (YTS), Ontario, Canada, taken at 0000 UTC 11 January 1998. The 6-hPa resolution of the sounding illustrates the intricate temperature, dewpoint, and wind structures that were present. The sounding shows a relatively deep boundary layer from the surface to 720 hPa, a weak inversion between 720 and 640 hPa, and a strong inversion at 640 hPa. Figure 5b shows a 24-h forecast sounding for YTS valid at 0000 UTC 11 January 1998 from the NCAR–PSU MM5 with-lake (WL) simulation that was run in real time during Lake-ICE. The WL model soundings were compared to corresponding no-lake (NL) model soundings to determine whether a lake aggregate event would take place. Sousounis and Fritsch (1994) describe in more detail the strategy and methodology behind conducting and comparing WL and NL simulations. A comparison of Figs. 5a,b indicates that most of the WL and CLASS sounding differences exist below 500 hPa. For example, the model sounding is too warm (and stable) between 800 and 620 hPa and too cold between 620 and 460 hPa. Additionally, the model sounding exhibits a weaker inversion between 800 and 700 hPa, less midlevel moisture, and fewer midlevel wind variations than the corresponding CLASS sounding. The fact that the largest differences exist at low levels suggests model deficiencies in boundary layer and/or convective processes. The presence of the lakes in the WL simulations suggests that the deficiencies are related to the heat and moisture flux parameterizations (Blackadar 1976) and the convective parameterization (Kain and Fritsch 1993) that were used in the model simulations.

Data from the other CLASS sites are plotted in Fig. 5c. Because the background flow during that IOP was relatively strong, the impact of the lake aggregate in southern Ontario appears at 900 hPa as a trough with cyclonic flow. It is useful to filter (remove) the large-scale flow in order to better visualize the cyclonic circulation induced by the lake aggregate. One way in which this filtering can be accomplished is by subtracting the NL soundings from the CLASS soundings that were taken during Lake-ICE. The NL simulation may legitimately be a better representation of what the situation would have been like without the lakes than the WL simulation is of reality because of the likely source of the WL errors. The CLASS–NL perturbation wind and temperature patterns in Fig. 5c indicate a closed cyclonic circulation and positive temperature perturbation just northeast of Lake Huron. The WL – NL differences are also shown for reference. The WL – NL wind differences also show a cyclonic circulation but with different characteristics. Given that both WL – NL and CLASS – NL wind differences, in general, at this time are light (< 3 m s^{-1}), the directional differences may not be as significant as they appear. A clearer picture of this event will exist after additional data (e.g., WSR-88D observed winds and operational upper-air profiles) are included in the analyses. These initial results suggest that the CLASS data taken in southeastern Canada during Lake-ICE will give valuable insight into the evolution of MAVs as well as into the accuracy of the model parameterizations of boundary layer and convective processes.

b. Lake-ICE example, 13 January 1998

The 13 January 1998 case was chosen to illustrate data taken by platforms close to Lake Michigan (Fig. 1). Widespread lake-effect clouds and snow were generated over Lake Michigan on this date following passage of a strong cold front the previous day (Fig. 6). Surface, aircraft, and satellite data suggest that the lake was approximately 15°–20°C warmer than the surface air temperatures near the upwind (western) shore.

The UW VIL showed micro-β-scale convective patterns within the surface layer over the water near the upwind shore (Fig. 7). These observations suggest an open cellular pattern with size scales of a few hundred meters. Downward motion in the clear middle areas of the cells appears to concentrate near-surface cloud droplets ("sea smoke") and the upward convective motion in thin boundaries between cells. The relationship between these micro-β-scale cells and the meso-γ-scale convective patterns observed at greater fetches over Lake Michigan is not understood.

NCAR ISS sites were located near the upwind and downwind shores of Lake Michigan, and farther inland from the downwind shore, to obtain data on the modification of air as it crossed the relatively warm lake. Figure 8 shows ISS rawinsonde soundings taken from these sites near 1630 UTC on 13 January 1998. The growth of the convective boundary layer across the lake is clear, with surface air temperatures increasing by nearly 8°C, an increase in moisture in the lowest 100 hPa of the atmosphere with changes up to nearly 850 hPa, and the growth of a convective layer from 960 hPa near the upwind shore to about 900 hPa near the downwind shore. Examples of data taken by in situ and remote-sensing techniques for this event are given in this section.

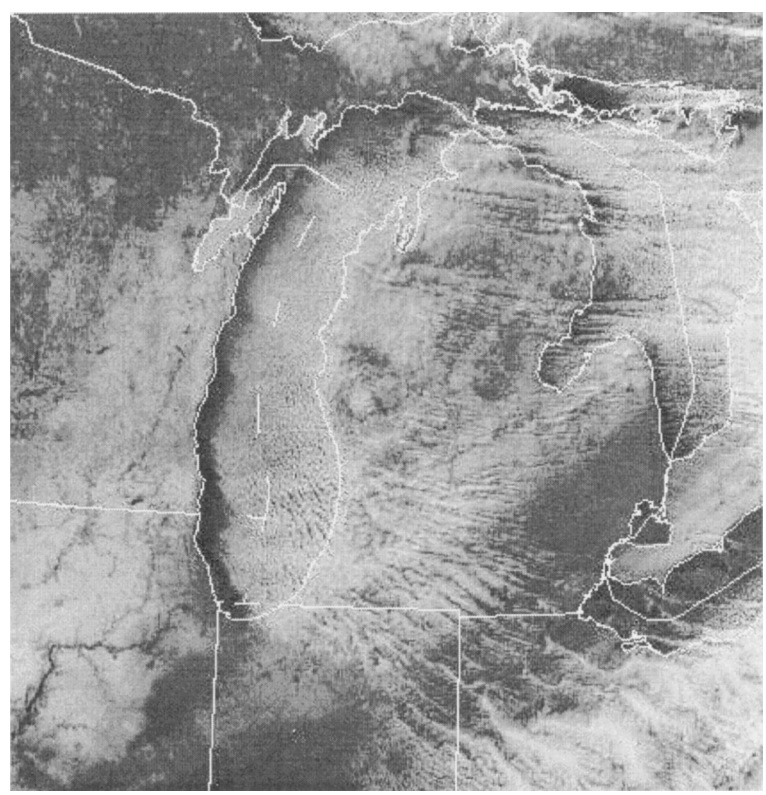

FIG. 6. *GOES-8* visible imagery taken at 1502 UTC on 13 Jan 1998.

1) Electra in situ data

Cross-lake flight legs conducted by the NCAR Electra on 13 January 1998 illustrate many of the details of the rate of airmass modification by surface fluxes and entrainment across Lake Michigan. The sample transect shown in Fig. 9 was flown from near the downwind (eastern) shore to near the upwind (western) shore of the lake at an altitude of about 735 m above the lake level (Fig. 1). The Electra flight tracks were nearly parallel to the wind direction (within about 20°). At this flight level, the aircraft passed from the midlevels of the deepest part of the lake-induced convective boundary layer, through the entrainment zone of the shallower, more upwind, parts of this boundary layer, and on into the free troposphere over the shallowest part of the boundary layer near the upwind shore. Thus, the downwind modification of the air over the lake can be examined by moving from right to left in Fig. 9.

The free troposphere at 735 m above lake level was relatively nonturbulent as seen in the limited amplitude of variations in vertical velocity, potential temperature, and mixing ratio for flight-leg times greater than 800 s. Between approximately 660 and 800 s, the aircraft passed through the entrainment zone (portion of the boundary layer where the turbulence dynamics is responding to both convection from below and the capping inversion above) of the lake-induced convective boundary layer. In this section of the flight leg, potential temperature decreased by over 2 K in the downwind direction while mixing ratio more than doubled. Vertical velocity variations in the entrainment zone were much greater than those in the free troposphere and only moderately less than those in the midlevels

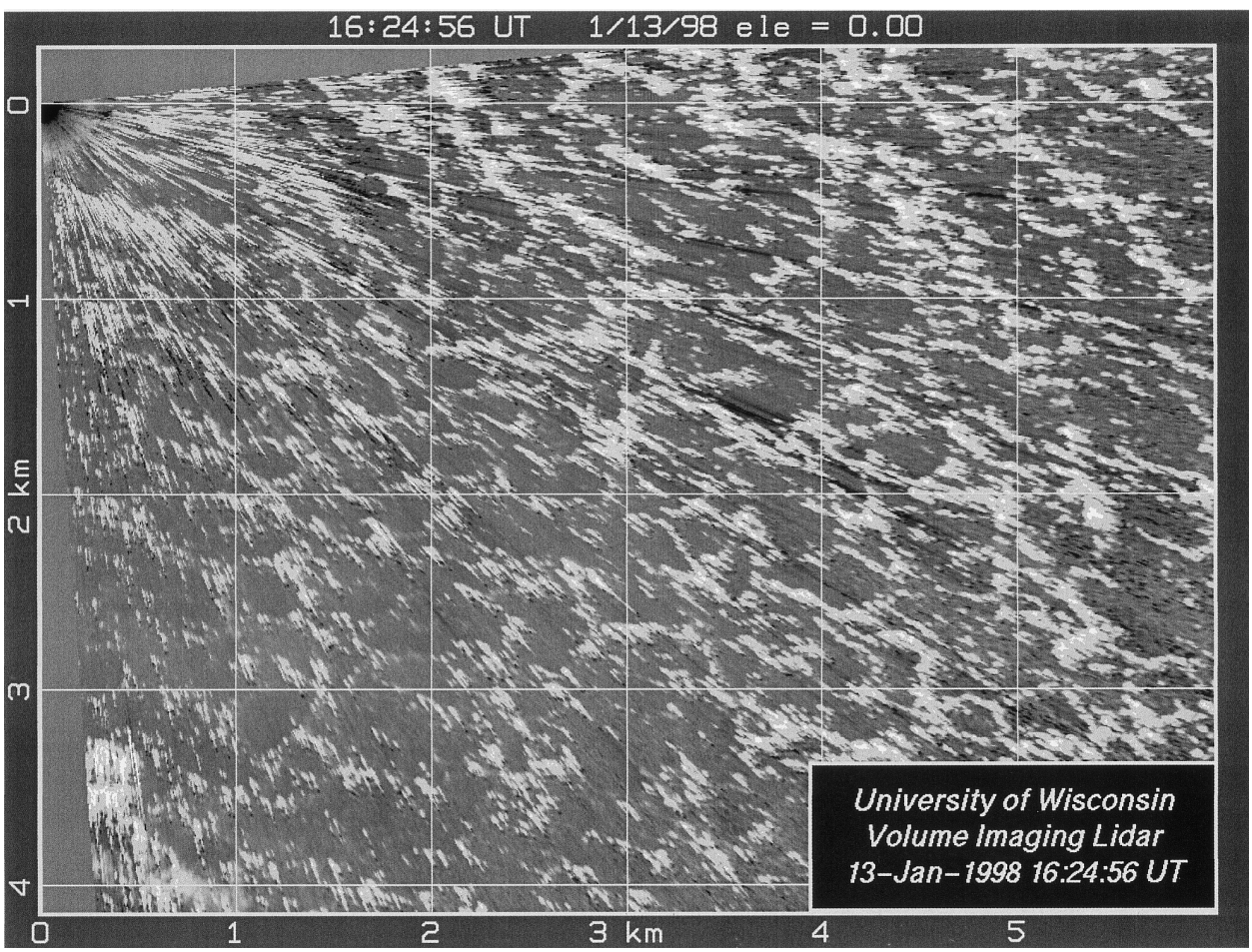

Fig. 7. A plan position indicator scan showing steam–fog patterns observed with the University of Wisconsin volume imaging lidar at 1625 UTC on 13 Jan 1998. The image shows structures 5 m above the surface in a 6 km × 6 km area directly downwind of the Sheboygan, WI, lakefront. Darker lines oriented along radials from the VIL are due to attenuation of the laser by brighter surface-layer features. VIL observations shown were taken with an azimuthal resolution of 0.08° and range resolution of 15 km.

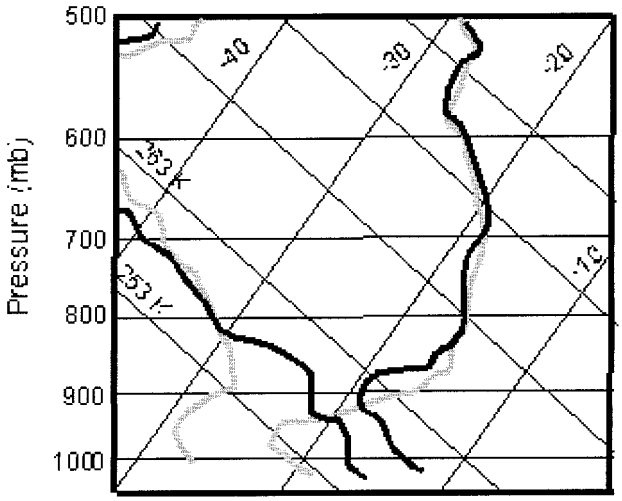

FIG. 8. NCAR ISS soundings taken upwind (Sheboygan, WI, gray lines) and downwind (Muskegon, MI, black lines) of Lake Michigan at about 1630 UTC on 13 Jan 1998.

this zone, both potential temperature and mixing ratio increased linearly with downwind distance. The relatively warm, moist updraft events responsible for this airmass modification can be seen most distinctly at the downwind end of the flight leg, for leg times less than 200 s. By the downwind shore of the lake, the air mass at flight level was about 3 K warmer and 3 to 4 times more moist than at the upwind shore. This setting provides sufficient convective intensity for study of both airmass modification and the microscale and mesoscale phenomena responsible for the change.

2) UNIVERSITY OF WYOMING KING AIR IN SITU DATA

The primary goal of the University of Wyoming King Air in Lake-ICE was to collect a dataset on turbulent, thermodynamic, and microphysical characteristics within the zone of ELDORA observations of

of the lake-induced convective boundary layer sampled farther downwind. These trends reflect the strong sensible flux divergence and moisture flux convergence at the top of the entrainment zone in this rapidly growing convective boundary layer. Thus, the Lake-ICE goal of sampling convective boundary layers with vigorous growth by entrainment, rather than encroachment, was achieved. Cloud fragments developed rapidly near the upwind shore (flight time 700 s) with about 500 droplets per cubic centimeter and 5–10 snow crystals per liter. Other evidence of rapid airmass modification is shown in the CN aerosol concentrations, which decreased steadily downwind due to scavenging and dilution.

Further downwind, between flight leg times 0 and 660 s, the boundary layer became increasingly deep relative to the flight level, leading to further intensification of the flight level vertical velocity variations and increasing skewness in favor of strong updraft events. The peak micro-γ-scale turbulent updraft/downdraft velocities were +5/–2.5 m s^{-1}. Throughout

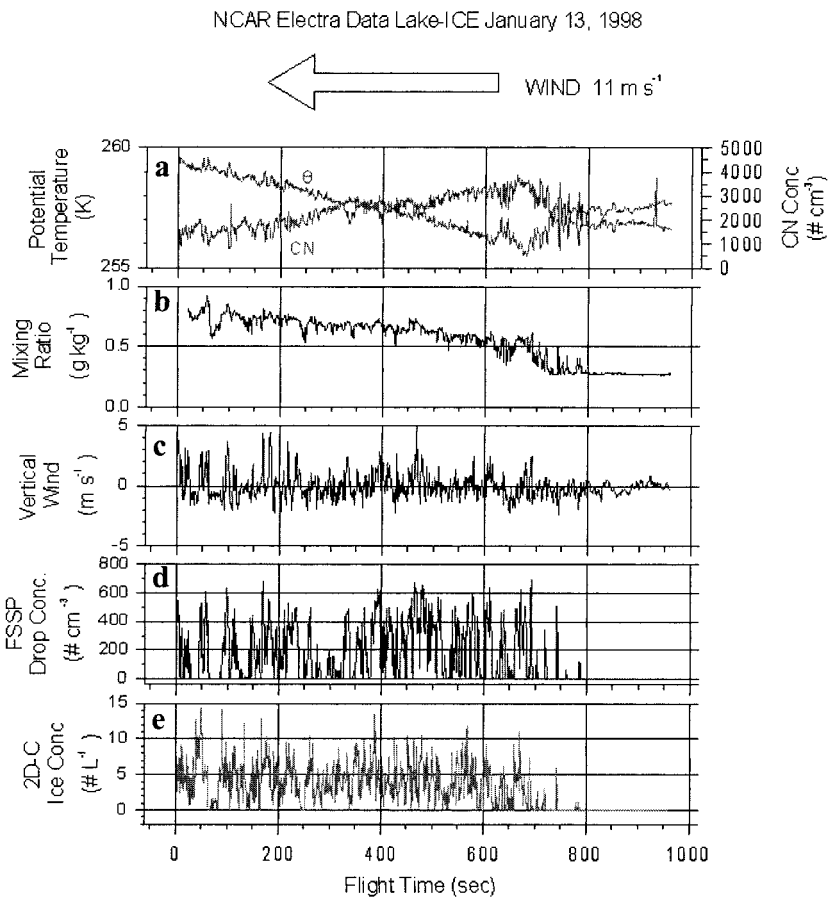

FIG. 9. In situ data taken by the NCAR Electra at 1409–1425 UTC on 13 Jan 1998. (a) Time series of potential temperature (K) and condensation nuclei concentration (cm^{-3}). (b) Vapor mixing ratio, as estimated by Lyman-α. (c) Vertical motions. (d) Cloud droplet concentration (cm^{-3}) measured by the FSSP. (e) Snowflake concentration (L^{-1}) as measured by the 2D-C probe. The aircraft was flying at near 735 m above the lake, toward the west (approximately into the wind).

meso-γ-scale convective structures. The King Air flight track generally consisted of three to four stacks of crosswind flight legs. The heights of the legs generally included samples within the cloud layer, in the entrainment zone, and above the boundary layer. Figure 10 gives time series of potential temperature, cloud-drop concentrations (uncorrected Particle Measuring Systems-FSSP total concentrations), and vertical velocities at three heights: 200 m (below cloud base), 700 m (near cloud base), and 1000 m (near cloud top) observed on 13 January 1998. All heights are in pressure altitude coordinates. These data were taken in the easternmost flight stack flown on this date (Fig. 1).

The data in Fig. 10 are typical of that expected in a convective boundary layer with internal clouds. Potential temperature time series at 200 m (Fig. 10e) show small-scale local peaks corresponding with convective updrafts (Fig. 10f). The mean potential temperature increases little from 200 m to near cloud base at 700 m (Fig. 10c), but increases by nearly 1 K between 700 and 1000 m (Fig. 10a). This increase is due to heating from both latent heat release and entrainment of relatively warm air from above the boundary layer top.

Cloud droplet concentrations occasionally peaked near 1500 cm^{-3} at both flight legs in the cloud layer. Note, however, that these concentrations are likely overestimates due to ice particle contamination (Gardner and Hallett 1985) and have not been corrected for the airspeed of the King Air, particle coincidence, or laser inhomogeneities (Dye and Baumgardner 1984; Baumgardner et al. 1985; Baumgardner and Spowart 1990). Near cloud base, increases in potential temperature correspond generally with locations of clouds as expected with moist convective plumes within the convective boundary layer. Near cloud top, convection overshot the level of neutral buoyancy, with clouds tending to correspond with locations of lower potential temperature.

Vertical motion observations illustrate well the convective nature of the boundary layer, with stronger motions measured at midlevels (700 m; Fig. 10d) than at either higher or lower levels (Figs. 10f,b). Vertical motions ranged from about +5.5 to –3.0 m s^{-1} at 700 m and were generally within about ±3 m s^{-1} at other levels. The distribution of vertical motions was positively skewed within the boundary layer (a few strong updrafts, many weak downdrafts), as expected with convective boundary layers. Data such as these show great promise in giving information on microscale processes embedded within the mesoscale convective structures observed by ELDORA.

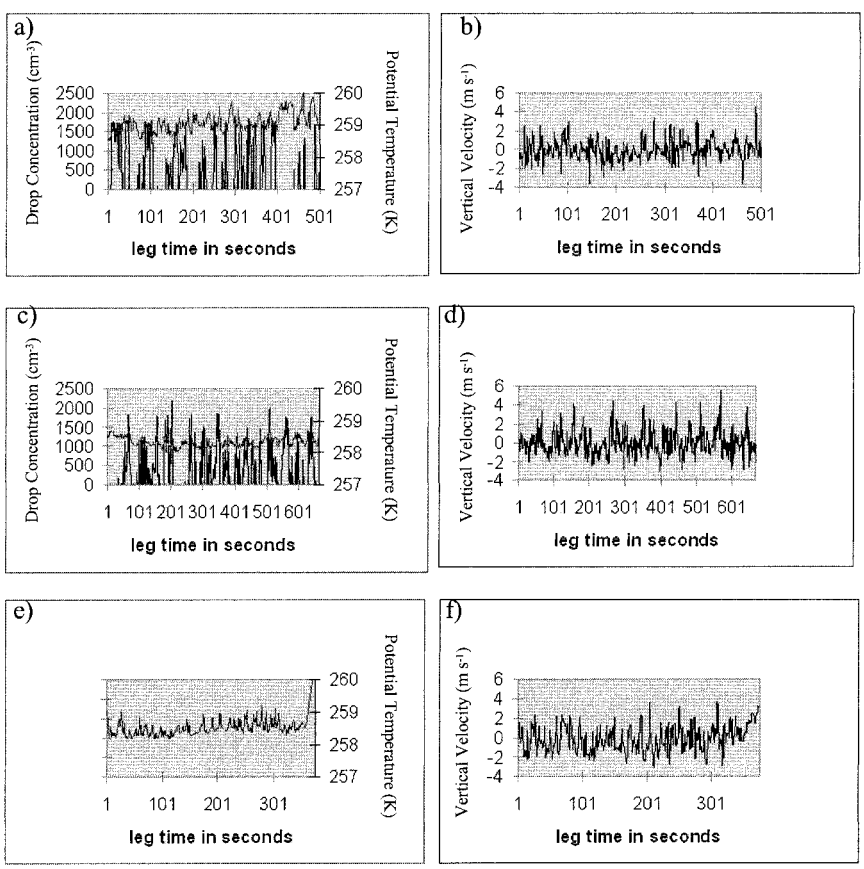

FIG. 10. In situ data taken by the University of Wyoming on 13 Jan 1998. (a) and (b) Potential temperature, cloud droplet concentrations (FSSP), and vertical motion time series at pressure altitude of 1000 m above the surface. (c) and (d) These observations at pressure altitude of 700 m. (e) and (f) Potential temperature and vertical motion at a pressure altitude of 200 m.

3) NCAR ELDORA DATA

One of the major goals of Lake-ICE was to determine the temporal and spatial evolution of meso-γ-scale circulations within lake-effect convective boundary layers and to determine mechanisms controlling their development. Observa-

tions taken by ELDORA, in combination with in situ aircraft observations and satellite images, give information on convective structures across much of Lake Michigan. This is critical especially over midlake where ground-based radars often overshoot the relatively shallow boundary layer. An example sweep of ELDORA measured reflectivity and relative winds (18° from the vertical) is given in Fig. 11. These data were taken at 1406 UTC on 13 January 1998. Radar sweeps, oriented roughly up–down through the boundary layer, indicate both upper-level divergence and low-level convergence. The white arrows in Fig. 11 (bottom panel) schematically indicate the location of the associated updraft, which is within the region of highest reflectivity (top panel).

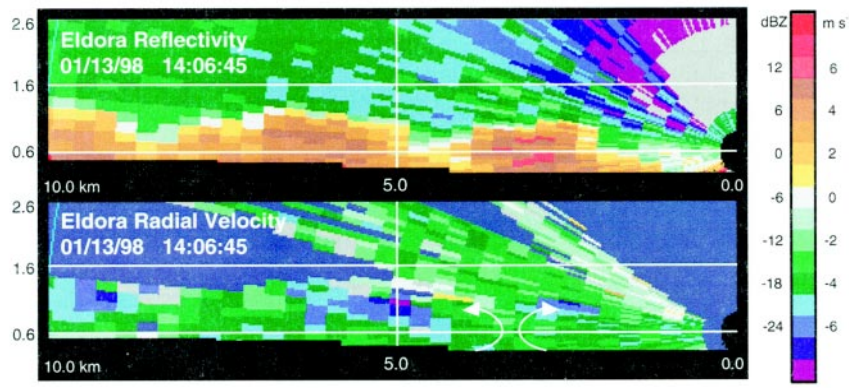

FIG. 11. Range–height display of effective reflectivity factor and radial velocity observations taken by the ELDORA at 1406 UTC on 13 Jan 1998. The aircraft was flying toward the ESE, approximately 20° to the left of the mean wind direction. This represents a near-vertical slice (18° forward of vertical) through the convective boundary layer, taken by the forward radar. White arrows indicate schematically the airflow associated with the observed near-surface convergence and higher-level divergence within the high-reflectivity region.

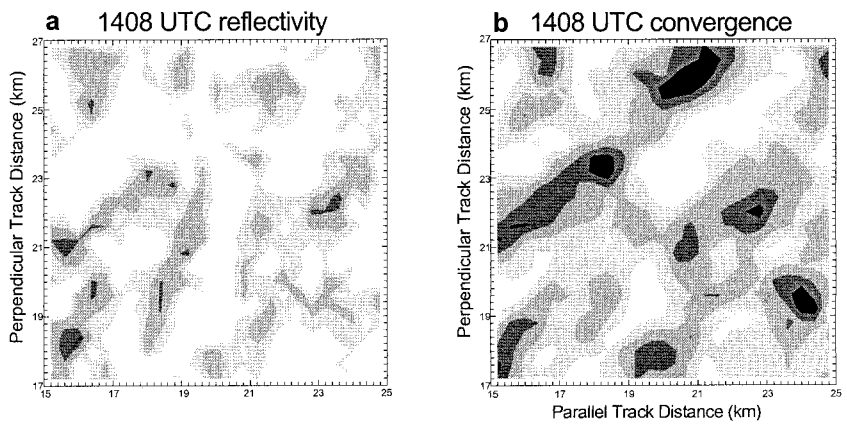

FIG. 12. ELDORA data interpolated to 0.9-km height (near the top of the convective boundary layer) at about 1408 UTC on 13 Jan 1998. Shown are (a) effective reflectivity factor and (b) convergence patterns. Dark shading indicates higher reflectivity and divergence.

Preliminary analyses of ELDORA data were accomplished using the NCAR software package SOLO for editing of radar data, REORDER for interpolation of these data to horizontal grids, and CEDRIC for wind syntheses (Hildebrand et al. 1996; Wakimoto et al. 1996). Observations taken by ELDORA were in good qualitative agreement with the available WSR-88D and satellite observations. Figure 12 shows an example 10 km × 10 km reflectivity (Fig. 12a) and associated convergence (Fig. 12b) field interpolated to 0.9-km height above lake surface. This height is near the top of the convective boundary layer. These data were taken within 15 km north of the NCAR Electra, at about 1408 UTC on 13 January 1998 near the middle of the lake.

As expected, the reflectivity pattern was quite random in appearance, with some indication of both along-wind and crosswind linear patterns. Interpolated wind fields were quite reasonable compared to King Air and surface observations. The convergence pattern shows good agreement with the reflectivity field, with higher reflectivity regions (darker shading in Fig. 12a) roughly collocated with divergence at upper levels in the boundary layer (darker shading in Fig. 12b). These observations indicate that the data are quite reasonable and, with proper care, will be able to resolve boundary layer convective circulations close to the aircraft path. These data show promise of giving quantitative information on the spatial and temporal evolution of meso-γ-scale convective patterns over Lake Michigan.

4) PSU COS DATA

The PSU COS was located near the downwind (eastern) shore of Lake Michigan to give detailed information on the vertical structure of clouds and precipitation within the lake-effect convective boundary layer. An example of observations taken as a cloud

band passed over the PSU COS on 13 January 1998 is displayed in Fig. 13. A time–height cross section from the vertical pointing cloud radar with the ceilometer-determined cloud base overlaid, an associated atmospheric temperature and dewpoint profile, and two velocity–power spectrographs are shown. Individual convective towers separated by lower reflectivity regions can be discerned within the larger banded structure. Several intense convective turrets penetrated approximately 200 m into the inversion. Two significant entraining events occurred at 1442 and 1449 UTC. The ceilometer cloud base varies substantially during this period, though most of the variability can be explained by the occurrence of intense snow showers. However, the general ceilometer cloud-base heights correspond well with that indicated by the sounding.

The velocity–power spectrographs show distributions of returned power as a function of velocity and height at a given instant in time. The velocity–power distribution at a given height is the familiar Doppler power spectrum, which, when integrated over the velocity interval, gives the reflectivity. Times for the two spectrographs are indicated on the time–height display. Spectrograph A was taken at the edge of one of the more intense convective events. Most of the atmospheric profile is characterized by upward velocities, as would be expected in the upward branch of a boundary layer roll. Two distinct spectral peaks are evident within the cloud layer (indicated by the lines). The uppermost peak is associated with a small cloud-particle mode, while the lower peak is associated with faster falling precipitation particles. Profile B was taken in an entrainment event in the roll. The physical situation is more complex. The time–height profile reveals snow from an approaching tower (to the left) at low levels, and weak precipitation falling from a (apparently) weaker decaying convective tower overhead. This interpretation corresponds well with the velocity signatures captured in the spectrograph. The cloud layer is characterized with a general weak uplift, while well below cloud base a general downdraft is indicated. Note the discrete shift in the Doppler spectrum right at cloud base, indicative of changes in the microphysical characteristics of the

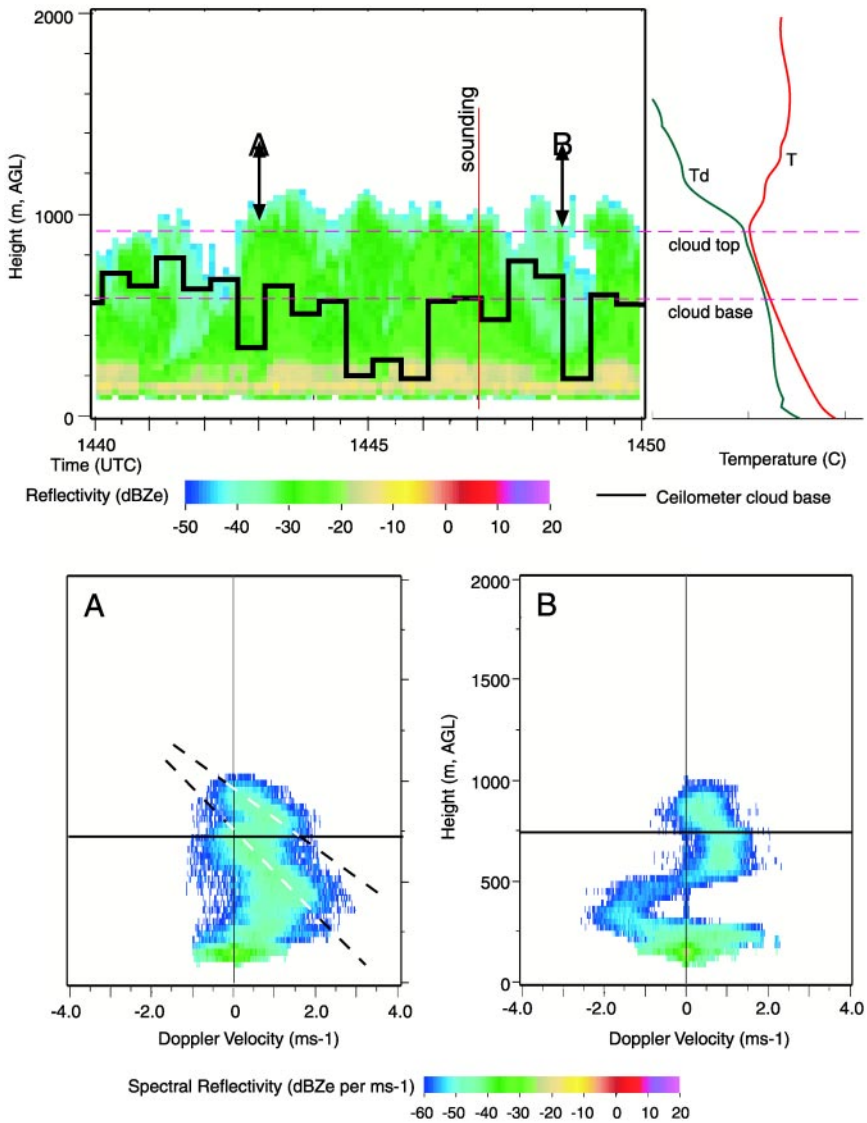

FIG. 13. Observations from the PSU COS of cloud band passing overhead. The top panel presents a time–height reflectivity plot derived from the vertically pointing 94-GHz radar with the ceilometer and cloud-base measurements overlaid and the temperature and dewpoint profile from the CLASS radiosonde system. The bottom panels show two velocity power spectrographs at the times A and B indicated on the time–height plot in the top panel. The dashed lines in the bottom left panel indicate estimates of the evolution of two spectral peaks, thought to represent the evolution of different types of hydrometeors.

scatterers. The lowest layers in all the images are contaminated by general low-level turbulence associated with surrounding towers and trees and cannot be physically interpreted. These figures reveal significant information on the micro-β-scale physical processes active in individual convective towers.

c. SNOWBAND, 8 January 1998

SNOWBAND conducted three IOPS: one addressing occlusion-sector snowband objectives (IOP-2), one addressing west shore lake-enhanced snowfall (IOP-9), and one addressing both objectives (IOP-5). In IOP-5, a series of four upper-level waves tracked northeastward from the Gulf of Mexico toward Canada. The last of these waves was accompanied by a surface cyclone that propagated from the Gulf Coast through east central Illinois. This cyclone later contributed to a devastating ice storm in northern New England and the Canadian provinces of Quebec and Ontario. Figure 14 shows 1-km resolution visible imagery at 1700 UTC on 8 January 1998 with a national infrared image inset. The flight track extended from the northernmost edge of the dry slot in the vicinity of northern Indiana to the northernmost edge of the heavy snow region in northeastern Wisconsin, crossing the rain–snow line. Nearly a foot of snow fell on the west shore of the lake. A remarkable feature in this storm was a very strong easterly low-level jet (Fig. 15) with a sharp velocity maximum of 35 m s^{-1} at 850 hPa in the middle of the warm frontal inversion. Extremely

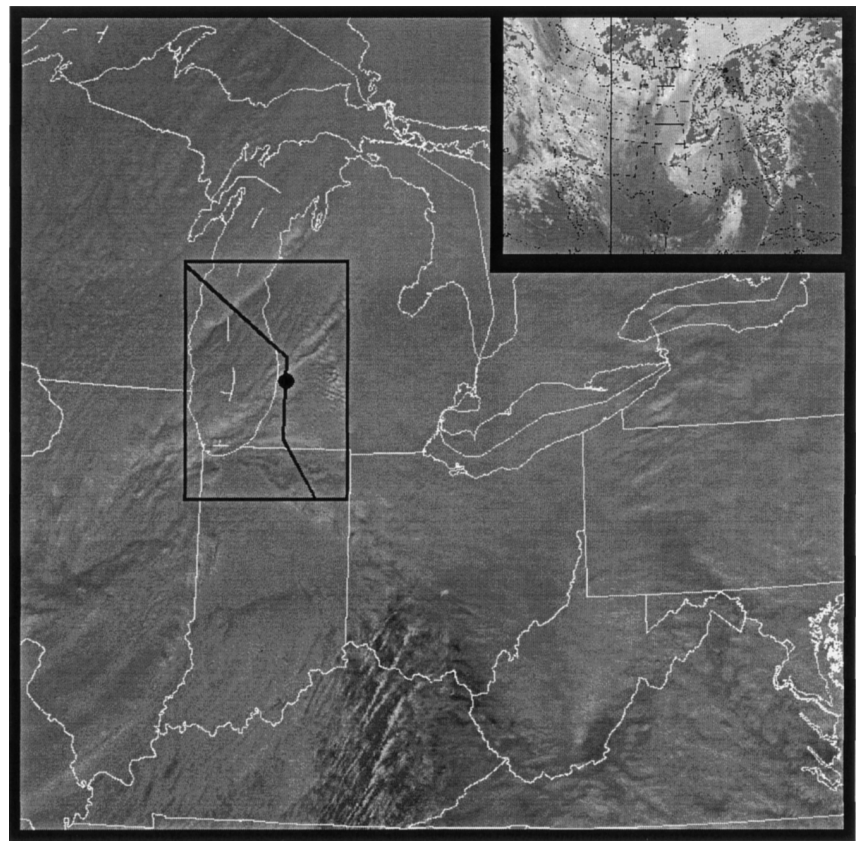

FIG. 14. 1-km resolution visible imagery at 1702 UTC on 8 Jan 1998 (image provided by NCAR/Research Applications Program). (Inset) Infrared image at the same time. The box and the Electra flight track (from 1451 to 1619 UTC) are for the time of the dual-Doppler syntheses shown in Fig. 16. The dot shows the location of the dropsonde launched at 1722 UTC, shown in Fig. 15.

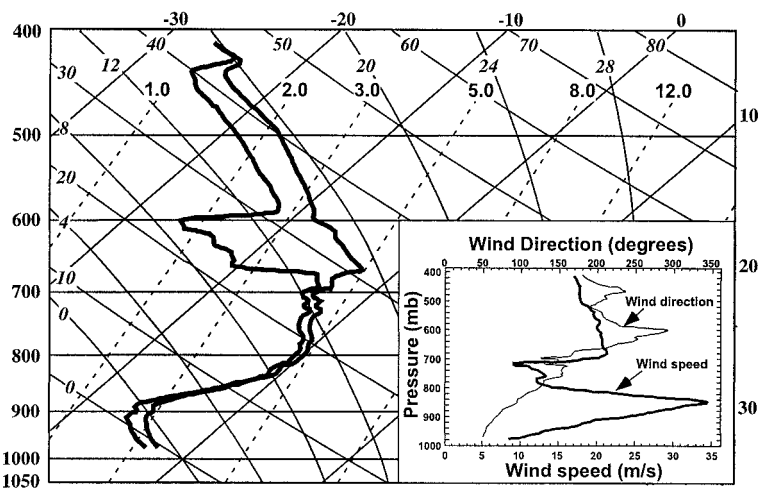

FIG. 15. Thermodynamic sounding from a dropsonde launched at the location shown in Fig. 14. The wind direction and speed are shown in the inset.

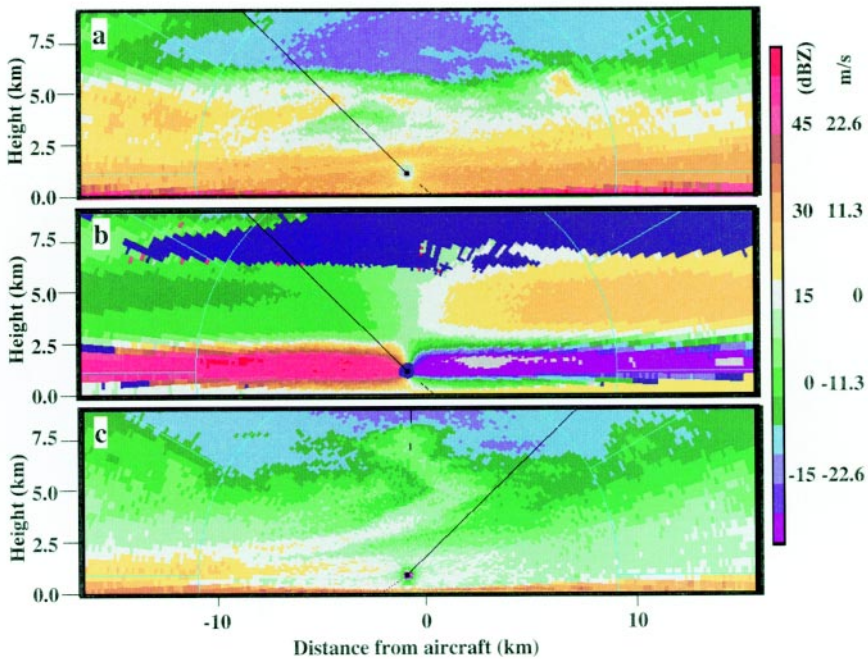

FIG. 16. ELDORA range–height indicator display of (a) equivalent reflectivity factor and (b) equivalent reflectivity factor at 1534 UTC on 8 Jan 1998, and (c) equivalent relativity factor at 1259 UTC on 21 Jan 1998.

strong shear was present both above and below the jet core. Figures 16a,b show the reflectivity and radial velocity structure measured by ELDORA in the vicinity of the jet. The aircraft is located at the dot at the center of the figure at about 1.2 km MSL. The data, from a 360° sweep of the aft radar of the ELDORA system, are presented in range–height indicator format. The band extended up to 7 km with the highest reflectivity below the frontal surface at 3 km. The frontal surface is marked by extremely strong shear. On the right (east) side of the diagram, strong inbound radial velocities (cold colors) are present below the front corresponding to the sharp easterly jet evident on Fig. 15. Aloft strong outbound radial velocities correspond to the westerlies above the front. Figure 17 shows a horizontal cross section of the reflectivity field and wind field in the snowband at 4.5 km. The winds are from a preliminary dual-Doppler synthesis. Two bands of higher reflectivity were present. In future syntheses, the winds within these bands will be determined at a vertical resolution of ~500 m, allowing a detailed analysis of their kinematic structure.

During IOP-2, a midlatitude cyclone propagated from the Oklahoma panhandle up the Ohio River valley, moving into central Ohio by midday on 10 December 1997. This system was characterized by pronounced isentropic lift and heavy snowfall in Michigan in a band northwest of the cyclone track. The aircraft mission included six passes across the heavy snowband from the dry slot over central Indiana to the northern edge of the band in Michigan. During the 6-h Electra flight, over 8 in. of snow fell at Ann Arbor, Michigan, closing Willow Run Airport, the base of the Electra operations, and forcing the aircraft to land at its alternate airport in Green Bay, Wisconsin. In IOP-2, only a single wide band was observed.

During IOP-9 on 21 January 1998, a cyclone propagated eastward from Kansas across Illinois and Indiana, producing a weak west shore lake-enhancement event. Nearly 6 in. of snow was reported at several locations in Wisconsin and Michigan. Figure 16c shows a cross section through a band southwest of the aircraft track as the aircraft flew west across Lake Michigan. An 18 m s^{-1} easterly jet centered at 900 hPa was present near the western shore of the lake at this time. The ELDORA reflectivity shows several examples of cells near cloud top seeding lower clouds confined below the frontal inversion.

The extremely high resolution measurements from SNOWBAND are confined to the local area of the aircraft flight. To permit interpretation of these mesoscale observations in the dynamic and thermodynamic context of the larger-scale weather systems, high-resolution modeling studies of the SNOWBAND cyclones will be carried out using the NCAR–PSU MM5 model. The observations will provide a clear basis for evaluating the model results. At the same time, the model fields will allow us to evaluate the dynamical processes producing the snowfall. Furthermore, the model will allow the calculation of detailed time-dependent trajectories, helping us complete our picture of cyclone-relative flow in the presence of active winter precipitation.

6. Collaborative efforts

In addition to the major focus of the project, there were several piggyback experiments utilizing the re-

sources that were assembled. Topics of these experiments were complementary but separate from the main thrust of the Lake-ICE and SNOWBAND projects.

a. Airborne ice nuclei measurements

A critical step in the precipitation process is the initiation of the ice phase. Colorado State University's (CSU) collaborative study involved performing aerosol particle measurements from the NCAR Electra. This study continues the CSU work on ice initiation in cold clouds, particularly through heterogeneous nucleation processes. The focus is to examine the relationship between ice-nucleating aerosol particles (IN) and the ice crystals that form in clouds by obtaining, simultaneously, measurements of IN and ice crystals.

The CSU ice nucleus instrument is a newly designed continuous-flow diffusion chamber (Rogers et al. 2000, manuscript submitted to *J. Atmos. Oceanic Technol.*). The sampling temperature and supersaturation are independently controlled. Active IN particles nucleate and grow to crystals of detectable size and are counted in real time. For selected time periods, these crystals can be impacted onto electron microscope grids for later examination of the size, chemical composition, and morphology of the nuclei (Chen et al. 1998), for studies of their composition and possible origin.

During Lake-ICE and SNOWBAND, the number concentration of IN was measured over a range of temperatures and humidities, spanning the expected thermodynamic conditions in the lake-effect clouds. Some fraction of the IN sampling was done in collaboration with University of Illinois investigators (Beard and Ochs 1986) to support their exploratory studies of the ice-nucleating properties of aerosols that are evaporated residues of cloud particles. These particles are isolated by the counterflow virtual impactor (Twohy et al. 1997) and were fed to the continuous-flow diffusion chamber.

The real-time ice nucleus instrument provides the capability to address key questions about ice formation by measuring ice nuclei in the inflow air of supercooled clouds as well as the concentration of ice crystals that subsequently form in the clouds. Although a Lagrangian parcel-following experiment would be ideal to address these questions, such experiments are difficult to execute and were not performed in this project. Nevertheless, the flight plans included many segments with along-wind passes at altitudes ranging from the lake's boundary layer, through the stratocumulus lake-effect clouds, and above. These flights provided a unique opportunity to study the microphysics of lake-effect cloud formation and evolution. Transit and ferry flight periods were also useful for measuring the vertical profiles and variability of aerosol particles.

In postproject analysis, IN and total aerosol data will be compared with in situ measurements of cloud ice concentration, as measured by the Electra's cloud

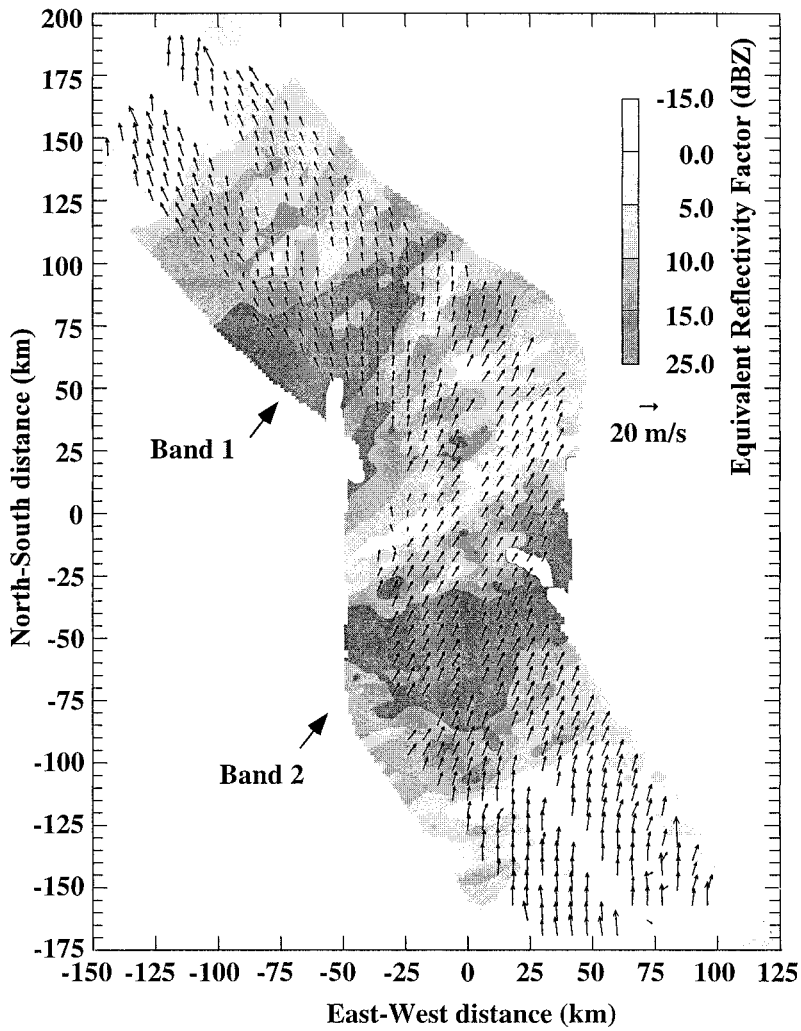

FIG. 17. Equivalent reflectivity factor and synthesized winds at 4.5-km altitude derived from a synthesis of radial velocities from the ELDORA fore and aft radars.

physics probes. These analyses will allow for examination of the connection between the activity of ice-nucleating aerosols and the presence of ice crystals in supercooled clouds. The goal of these studies is to infer the modes of ice formation (Vali 1985), to describe spatial distributions of IN and aerosols, and to indicate possible source regions and transformation processes. This information has important applications in conceptual and numerical cloud-modeling studies.

b. Airborne cloud drop charge measurements

The purpose of the drop charge measurements in the Lake-ICE and SNOWBAND field projects was to obtain spatial and temporal data for analysis with concurrent measurements of other cloud parameters. For these aircraft measurements of drop charge, the cloud drops were sampled and evaporated using a counterflow virtual impactor in cooperation with C. Twohy. The drop residue was collected by an absolute filter electrometer having a sensitivity of 1 femtoamp (10^{-15} A).

Preliminary data analysis of flights through stratocumulus clouds over Lake Michigan showed positive drop charges near cloud top with the highest values at cloud edges. The drop charges appear to have originated from space charge that accumulates at cloud edge because of different conductivities in clear and cloudy air (e.g., Beard and Ochs 1986). Negative drop charges were found below cloud top throughout the stratocumulus layer. The polarity appears to be associated with buoyant parcels that have ascended from cloud base where the space charge is negative. Descending, clear-air parcels originating near cloud top should contain positive charges that can be evaluated from separate measurements of aerosol charge. The observations of charges on drops and aerosols in stratocumulus clouds will help guide research in the Cloud Physics Laboratory at the Illinois State Water Survey on the effects of charge in promoting drop collisions and enhancing ice nucleation (e.g., Beard 1992; Tinsley et al. 2000).

7. Summary

One of the most difficult tasks in meteorology is to understand how processes that occur over a very wide range of size and timescales interact to produce severe weather. The Lake-Induced Convection Experiment (Lake-ICE) and the Snowband Dynamics Project (SNOWBAND) collected an extensive dataset on two types of severe winter events: lake-effect snowstorms and heavy snowbands associated with cyclones. Over a 2-month period in the winter of 1997/98, intensive observations were taken during lake-effect storms and cyclones in the Great Lakes region in order to better understand the various scales of phenomena involved in each of these wintertime events.

This paper describes the major objectives and operations of the Lake-ICE and SNOWBAND projects and gives examples of the state-of-the-art data collected during the projects. The overall goals of Lake-ICE were to develop a better understanding of meso-α-scale aggregate vortices, meso-γ-scale boundary layer circulations, and interactions between mesoscale circulations and turbulent micro-γ-scale mixing processes throughout the convective boundary layer in lake-effect snow events. SNOWBAND sought to develop a better understanding of bands of heavy precipitation in the northwest quadrant of cyclones and of enhancement of precipitation associated with cyclones over the Great Lakes.

Preliminary data presented suggest that these field projects resulted in an exceptionally complete, high quality dataset on lake-effect storm and cyclone processes, convective boundary layer circulations, and mesoscale dynamics.

Acknowledgments. This project was sponsored by the National Science Foundation under grants NSF ATM 97-07165, 97-08170, 97-07730, 97-08314, 98-13398, 98-16203, 98-16306, 96-29567, 96-29343, 95-02009, 95-05298, and 97-14177. Additional funds were provided by Army DAAH 04-94-G-0022, SUNY—Brockport, and the Lucia Harrison Endowment Fund at Western Michigan University. The authors of this manuscript are very grateful for the efforts of the NCAR and University of Wyoming facilities teams (facilities managers, scientists, engineers, pilots, etc.). These projects would not have been successful without the extensive efforts of these staff members. We also appreciate the help of students and staff from the 22 institutions involved in this project. Mr. Greg Mann (University of Michigan) and Mr. Brad Hoggatt (University of Wisconsin) were lead forecasters throughout the field experiment. Without the help of a large number of volunteers and employees, Lake-ICE and SNOWBAND would not have been nearly as successful. Primary publication costs for this manuscript were paid by NSF Grant ATM 98-16306. Comments of the anonymous reviewers are greatly appreciated.

References

Agee, E. M., and M. L. Hart, 1990: Boundary layer and mesoscale structure over Lake Michigan during a wintertime cold air outbreak. *J. Atmos. Sci.,* **47,** 2293–2316.

Albrecht, B. A., T. P. Ackerman, G. G. Mace, D. W. Thomson, M. A. Miller, and R. M. Peters, 1991: A surface cloud observing system. Preprints, *Seventh Conf. on Meteorological Observations and Instrumentation,* New Orleans, LA, Amer. Meteor. Soc., 443–446.

Angel, J. R., and S. A. Isard, 1997: An observational study of the influence of the Great Lakes on the speed and intensity of passing cyclones. *Mon. Wea. Rev.,* **125,** 2228–2237.

Atlas, D., B. Walker, S.-H. Chou, and P. J. Sheu, 1986: The structure of the unstable marine boundary layer viewed by lidar and aircraft observations. *J. Atmos. Sci.,* **43,** 1301–1318.

Bates, G. T., F. Giorgi, and S. W. Hostetler, 1993: Toward the simulation of the effects of the Great Lakes on regional climate. *Mon. Wea. Rev.,* **121,** 1373–1387.

——, S. W. Hostetler, and F. Giorgi, 1995: Two-year simulation of the Great Lakes region with a coupled modeling system. *Mon. Wea. Rev.,* **123,** 1505–1553.

Baumgardner, D., and M. Spowart, 1990: Evaluation of the forward scattering spectrometer probe. Part III: Time response and laser inhomogeniety limitations. *J. Atmos. Oceanic Technol.,* **7,** 666–672.

——, W. Strapp, and J. E. Dye, 1985: Evaluation of the Forward Scattering Spectrometer Probe. Part II: Corrections for coincidence and dead-time losses. *J. Atmos. Oceanic Technol.,* **2,** 626–632.

Beard, K. V., 1992: Ice initiation in warm-base cumulus clouds: An assessment of microphysical mechanisms. *Atmos. Res.,* **28,** 125–152.

——, and H. T. Ochs, 1986: Charging mechanisms in clouds and thunderstorms. *The Earth's Electrical Environment,* National Academy Press, 114–130.

Blackadar, A. K., 1976: High resolution models of the planetary boundary layer. *Advances in Environmental Science and Engineering,* Pfafflin and Ziegler, Eds., Vol. 1, Gordon and Breach Science, 50–85.

Caulliez, G., N. Ricci, and R. Dupont, 1998: The generation of the first visible wind waves. *Phys. Fluids,* **10,** 757–759.

Changnon, S. A., cited 1999: January 1999 Blizzard. Impacts of the New Years 1999 Blizzard in the Midwest. [Available online at http://www.ncdc.noaa.gov/ol/climate/extremes/1999/january/blizzard99.html.]

Chen, Y., S. M. Kreidenweis, L. M. McInnes, D. C. Rogers, and P. J. DeMott, 1998: Single particle analyses of ice nucleating aerosols in the upper troposphere and lower stratosphere. *Geophys. Res. Lett.,* **25,** 1391–1394.

Christian, T. W., and R. M. Wakimoto, 1989: The relationship between radar reflectivities and clouds associated with horizontal roll convection on 8 August 1982. *Mon. Wea. Rev.,* **117,** 1520–1544.

Cox, H. J., 1917: Influence of the Great Lakes upon movement of high and low pressure areas. *Proc. Second Pan Amer. Sci. Congr.,* **2,** 432–459.

Dalu, G. A., and R. A. Pielke, 1993: Vertical heat fluxes generated by mesoscale atmospheric flow induced by thermal inhomogeneities in the PBL. *J. Atmos. Sci.,* **50,** 919–926.

Dorman, C. E., and E. Mollo-Christensen, 1973: Observation of the structure on moving gust patterns over a water surface ("cat's paws"). *J. Phys. Oceanogr.,* **3,** 120–132.

Dye, J. E., and D. Baumgardner, 1984: Evaluation of the Forward Scattering Spectrometer Probe. Part I: Electronic and optical studies. *J. Atmos. Oceanic Technol.,* **1,** 329–344.

Gardner, B. A., and J. Hallett, 1985: Degradation of in-cloud Forward Scattering Spectrometer Probe measurements in the presence of ice particles. *J. Atmos. Oceanic Technol.,* **2,** 171–180.

Hildebrand, P. H., and Coauthors, 1996: The ELDORA/ASTRAIA airborne Doppler weather radar: High-resolution observations from TOGA COARE. *Bull. Amer. Meteor. Soc.,* **77,** 213–232.

Hjelmfelt, M., 1990: Numerical study of the influence of environmental conditions on lake-effect snowstorm on Lake Michigan. *Mon. Wea. Rev.,* **118,** 138–150.

Johannessen, J. A., R. A. Shuchman, O. M. Johannssen, K. L. Davidson, and D. R. Lyzenga, 1991: Synthetic aperture radar imaging of upper ocean circulation features and wind fronts. *J. Geophys. Res.,* **96** (10), 411–422.

Kahma, K. K., and M. A. Donelan, 1987: A laboratory study of the minimum wind speed for wind wave generation. *J. Fluid Mech.,* **192,**339–364.

Kain, J. S., and J. M. Fritsch, 1993: The role of the convective "trigger function" in numerical prediction of mesoscale convective systems. *Meteor. Atmos. Phys.,* **49,** 93–106.

Kelly, R. D., 1984: Horizontal roll and boundary-layer interrelationships observed over Lake Michigan. *J. Atmos. Sci.,* **41,** 1816–1826.

——, 1986: Mesoscale frequencies and seasonal snowfalls for different types of Lake Michigan snowstorms. *J. Climate Appl. Meteor.,* **25,** 308–312.

Khalsa, S. J. S., 1993: Direct sampling of entrainment events in a marine stratocumulus layer. *J. Atmos. Sci.,* **50,** 1734–1750.

Kreitzberg, C. W., and H. A. Brown, 1970: Mesoscale weather systems within an occlusion. *J. Appl. Meteor.,* **9,** 417–432.

Kristovich, D. A. R., 1991: The three-dimensional flow fields of boundary layer rolls observed during lake-effect snow storms. Ph.D. thesis, University of Chicago, 178 pp.

——, 1993: Mean circulations of boundary-layer rolls in lake-effect snow storms. *Bound.-Layer Meteor.,* **63,** 293–315.

——, 1995: Profiles of moisture fluxes in snow-filled boundary layers. Preprints, *Conf. on Cloud Physics,* Dallas, TX, Amer. Meteor. Soc., 278–281.

——, and R. Steve, 1995: Lake-effect cloud band frequencies over the Great Lakes. *J. Appl. Meteor.,* **34,** 2083–2090.

——, and R. R. Braham Jr., 1998: Mean profiles of moisture fluxes in snow-filled boundary layers. *Bound.-Layer Meteor.,* **87,** 195–215.

Kunkel, K. E., R. A. Pielke Jr., and S. A. Changnon, 1999: Temporal fluctuations in weather and climate extremes that cause economic and health impacts: A review. *Bull. Amer. Meteor. Soc.,* **80,** 1077–1098.

Lavoie, R. L., 1972: A mesoscale numerical model of lake-effect storms. *J. Atmos. Sci.,* **29,** 1025–1040.

LeMone, M. A., 1976: Modulation of turbulence energy by longitudinal rolls in an unstable planetary boundary layer. *J. Atmos. Sci.,* **33,** 1308–1320.

——, and W. T. Pennell, 1976: The relationship of trade wind cumulus distribution to subcloud layer fluxes and structure. *Mon. Wea. Rev.,* **104,** 524–539.

Lenschow, D. H., P. B. Krummel, and S. T. Siems, 1999: Measuring entrainment, divergence, and vorticity on the mesoscale from aircraft. *J. Atmos. Oceanic Technol.,* **16,** 1384–1400.

MacVean, M. K., and P. J. Mason, 1990: Cloud-top entrainment instability through small-scale mixing and is parameterization in numerical models. *J. Atmos. Sci.,* **47,** 1012–1030.

Mahrt, L., and W. Gibson, 1992: Flux decomposition into coherent structures. *Bound.-Layer Meteor.,* **60,** 143–168.

Mann, G. E., 1999: Great Lakes collective influences upon the evolution of lake-effect storms in the western Great Lakes. Ph.D. thesis, University of Michigan, 285 pp.

Martin, J. E., 1998: The structure and evolution of continental winter cyclone. Part II: Frontal forcing for an extreme snow event. *Mon. Wea. Rev.,* **126,** 329–348.

——, 1999: Quasigeostrophic forcing of ascent in the occluded sector of cyclones and the trowal airstream. *Mon. Wea. Rev.,* **127,** 70–88.

Melfi, S. H., J. D. Spinhirne, S.-H. Chou, and S. P. Palm, 1985: Lidar observations of vertically organized convection in the planetary boundary layer over the ocean. *J. Climate Appl. Meteor.,* **24,** 806–821.

Moeng, C.-H., and P. P. Sullivan, 1994: A comparison of shear and buoyancy-driven planetary boundary layer flows. *J. Atmos. Sci.,* **51,** 999–1022.

Mourad, P. D., 1996: Inferring multiscale structure in atmospheric turbulence using satellite-based SAR imagery. *J. Geophys. Res.,* **101,** 18 433–18 449.

——, 1999: Footprints of atmospheric turbulence in synthetic aperture radar images of the ocean surface: A review. *Air–Sea Exchange—Physics, Chemistry, Dynamics, and Statistics,* G. L. Geernaert, Ed., Kluwer Academic, 269–290.

——, and B. A. Walter, 1996: Viewing a cold air outbreak using satellite-based synthetic aperture radar and advanced very high resolution radiometer imagery. *J. Geophys. Res.,* **101,** 391–400.

Moyer, K. A., and G. S. Young, 1991: Observations of vertical velocity skewness within the marine stratocumulus-topped boundary layer. *J. Atmos. Sci.,* **48,** 403–409.

NCAR Research Aviation Facility, 1997: *Bulletin 4.*

Niziol, T. A., 1987: Operational forecasting of lake effect snowfall in western and central New York. *Wea. Forecasting,* **2,** 310–321.

Orlanski, J., 1975: A rational subdivision of scales for atmospheric processes. *Bull. Amer. Meteor. Soc.,* **56,** 527–530.

Passarelli, R. E., Jr., and R. R. Braham Jr., 1981: The role of the winter land breeze in the formation of Great Lake snow storms. *Bull. Amer. Meteor. Soc.,* **62,** 482–491.

Petterssen, S., and P. A. Calabrese, 1959: On some weather influences due to the warming of the air by the Great Lakes in winter. *J. Meteor.,* **16,** 646–652.

Plant, W. J., 1990: Bragg scattering of electromagnetic waves from the air/sea interface. *Remote Sensing,* Geernaert and W. J. Plant, Eds., Vol. II, *Surface Waves and Fluxes,* Kluwer Academic, 41–109.

Rothrock, H. J., 1969: An aid in forecasting significant lake snows. Environmental Science Services Administration Tech. Memo. WBTM CR-30, 12 pp. [Available from NOAA/NWS, Central Region Headquarters, 601 E. 12th St., Kansas City, MO 64106.]

Schmidlin, T. W., and J. Kosarik, 1999: A record Ohio snowfall during 9–14 November 1996. *Bull. Amer. Meteor. Soc.,* **80,** 1107–1116.

Schultz, D. M., and C. F. Mass, 1993: The occlusion process in a midlatitude cyclone over land. *Mon. Wea. Rev.,* **121,** 918–940.

Scott, R. W., and F. A. Huff, 1996: Impacts of the Great Lakes on regional climate conditions. *J. Great Lakes Res.,* **22,** 845–863.

Shy, S. S., and R. E. Breidenthal, 1990: Laboratory experiments on the cloud-top entrainment instability. *J. Fluid Mech.,* **214,** 1–15.

Sikora, T. D., G. S. Young, R. C. Beal, and J. B. Edson, 1995: Use of spaceborne synthetic aperture radar imagery of the sea surface in detecting the presence and structure of the convective marine atmospheric boundary layer. *Mon. Wea. Rev.,* **123,** 3623–3632.

Sousounis, P. J., 1997: Lake-aggregate mesoscale disturbances. Part III: Description of a mesoscale aggregate vortex. *Mon. Wea. Rev.,* **125,** 1111–1134.

——, and J. M. Fritsch, 1994: Lake-aggregate mesoscale disturbances. Part II: A case study of the effects on regional and synoptic-scale weather systems. *Bull. Amer. Meteor. Soc.,* **75,** 1793–1811.

Streten, N. A., 1975: Cloud cell size and pattern evolution in Arctic air advection over the North Pacific. *Arch. Meteor., Geophys. Bioklimatol.,* **24A,** 213–228.

Tinsley, B. A., R. P. Rohrbaugh, M. Hei, and K. V. Beard, 2000: Effects of image charges on the scavenging of aerosol particles by cloud droplets and possible consequences for droplet charging and ice nucleation. *J. Atmos. Sci.,* in press.

Twohy, C. H., A. J. Schanot, and W. A. Cooper, 1997: Measurement of condensed water content in liquid and ice clouds using anairborne counterflow virtual impactor. *J. Atmos. Oceanic Technol.,* **14,** 197–202.

Vachon, P. W., I. Chunchuzov, and F. W. Dobson, 1998: Wind field structure and speed from RADARSAT SAR images. *Earth Observ. Quart.,* **59,** 12–15.

Vali, G., 1985: Nucleation terminology. *J. Aerosol Sci.,* **16,** 575–576.

Wakimoto, R. M., W.-C. Lee, H. B. Bluestein, C.-H. Liu, and P. H. Hildebrand, 1996: ELDORA observations during VORTEX 95. *Bull. Amer. Meteor. Soc.,* **77,** 1465–1481.

Wang, Q., and B. A. Albrecht, 1994: Observations of cloud-top entrainment in marine stratocumulus clouds. *J. Atmos. Sci.,* **51,** 1530–1547.

Weiss, C. C., and P. J. Sousounis, 1999: A climatology of collective lake disturbances. *Mon. Wea. Rev.,* **127,** 565–574.

Yuen, L. W., and J. A. Young, 1986: Dynamical adjustment theory for boundary layer flow in cold surges. *J. Atmos. Sci.,* **43,** 3089–3108.

Zishka, K. M., and P. J. Smith, 1980: The climatology of cyclones and anticyclones over North America and surrounding ocean environs for January and July, 1950–77. *Mon. Wea. Rev.,* **108,** 387–401.